Biomedicine & Pharmacotherapy 183 (2025) 117839

Contents lists available at ScienceDirect

Biomedicine & Pharmacotherapy

journal homepage: www.elsevier.com/locate/biopha

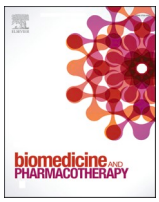

Colistin treatment causes neuronal loss and cognitive impairment via ros accumulation and neuronal plasticity alterations

Laura Guzman [a,b,c], Antoni Parcerisas [d,e,f,g], Amanda Cano [c,h], Elena Sánchez-López [c,i,j], Ester Verdaguer [b,c,k], Carme Auladell [b,c,k], Yolanda Cajal [i,j], Marta Barenys [a,l,m], Antoni Camins [a,b,c,n], Francesc Rabanal [o], Miren Ettcheto [a,b,c,n,*]

[a] Departament de Farmacologia, Toxicologia i Química Terapèutica, Facultat de Farmàcia i Ciències de l'Alimentació, Universitat de Barcelona (UB), Av. de Joan XXIII, 27-31, Barcelona 08028, Spain
[b] Institut de Neurociències, Universitat de Barcelona (UB), Passeig de la Vall d'Hebron, 171, Barcelona 08035, Spain
[c] Centro de Investigación Biomédica en Red Enfermedades Neurodegenerativas (CIBERNED), Instituto de Carlos III, Av. Monforte de Lemos, 3-5, Madrid 28029, Spain
[d] Tissue Repair and Regeneration Laboratory (TR2Lab), Institut de Recerca i Innovació en Ciències de la Vida i de la Salut a la Catalunya Central (IRIS-CC) Ctra. de Roda, 70, Vic 08500, Spain
[e] Universitat de Vic – Universitat Central de Catalunya (UVic-UCC), Sagrada Família, 7, Vic 08500, Spain
[f] Facultat de Ciències, Tecnologia i Enginyeria, Sagrada Família, 7, Vic 08500, Spain
[g] Departament de Biociències, Sagrada Família, 7, Vic 08500, Spain
[h] Ace Alzheimer Center Barcelona, C/Marquès de Sentmenat, 57, Barcelona 08029, Spain
[i] Departament de Farmàcia, Tecnologia Farmacèutica i Fisicoquímica, Facultat de Farmàcia i Ciències de l'Alimentació, Universitat de Barcelona (UB), Av. de Joan XXIII, 27-31, Barcelona 08028, Spain
[j] Institut de Nanociència i Nanotecnologia (IN2UB), Universitat de Barcelona (UB), Av. Diagonal, 64, Barcelona 08028, Spain
[k] Departament de Biologia Cel·lular, Fisiologia i Immunologia, Facultat de Biologia, Universitat de Barcelona (UB), Av. de Joan XXIII, 27-31, Barcelona 08028, Spain
[l] Institut de Recerca en Nutrició i Seguretat Alimentària (INSA), Universitat de Barcelona (UB), Av. Prat de la Riba, 171, Barcelona 08921, Spain
[m] German Centre for the Protection of Laboratory Animals (Bf3R), German Federal Institute for Risk Assessment (BfR), Germany
[n] Institut d'Investigació Sanitària Pere Virgili (IISPV), Hospital Universitari Sant Joan de Reus, Av. Josep Laporte, 2, Reus 43204, Spain
[o] Secció de Química Orgànica, Departament de Química Inorgànica i Orgànica, Facultat de Química, Universitat de Barcelona (UB), C/Martí i Franquès, 1-11, Barcelona 08028, Spain

ARTICLE INFO

Keywords:
Polymyxins
Colistin
Neurotoxicity
Hippocampus
Dendritic spines
Neurogenesis
Cognition

ABSTRACT

The rise of antimicrobial resistance has made necessary the increase of the antibacterial arsenal against multidrug-resistant bacteria. In this context, colistin has re-emerged as a first-line antibiotic in critical situations despite its nephro- and neuro- toxicity at peripheral level. However, the mechanism underlying its toxicity remains unknown, particularly in relation to the central nervous system (CNS). Therefore, this study aimed to characterize the molecular mechanisms underlying colistin-induced neurotoxicity in the CNS through a combination of *in vitro* and *in vivo* molecular studies along with several *in vivo* behavioral tests. Following colistin treatment, mice exhibited a significant reduction in body weight together with renal impairment, and locomotor dysfunction. Moreover, our results demonstrated that colistin disrupted the blood-brain barrier, inducing astrogliosis, and triggering apoptosis-related processes probably through the accumulation of reactive oxygen species (ROS) and mitochondrial dysfunction. Further analysis on mice and primary neuronal cultures revealed that colistin administration altered neuronal plasticity by reducing the number of immature neurons in adult neurogenesis and altering the synaptic function through a reduction of the post-synaptic protein PSD95. All these alterations together finally lead to cognitive impairment and depression-like symptoms in mice. These findings provide novel insights into the mechanisms of colistin-induced neurotoxicity in the CNS, highlighting the need for careful monitoring of cognitive function in patients undergoing colistin treatment.

* Correspondence to: Department of Pharmacology, Toxicology and Therapeutic Chemistry, Faculty of Pharmacy and Food Sciences, University of Barcelona, Institut de Neurociencies (UBneuro), University of Barcelona, Biomedical Research Networking Centre in Neurodegenerative Diseases (CIBERNED), Avda/Joan XXIII, Barcelona, Madrid, Spain.
E-mail address: mirenettcheto@ub.edu (M. Ettcheto).

https://doi.org/10.1016/j.biopha.2025.117839
Received 12 November 2024; Received in revised form 31 December 2024; Accepted 9 January 2025
Available online 16 January 2025
0753-3322/© 2025 Published by Elsevier Masson SAS. This is an open access article under the CC BY-NC-ND license (http://creativecommons.org/licenses/by-nc-nd/4.0/).

1. Introduction

Antimicrobial resistance (AMR) is one of the biggest problems that humanity is currently facing, and it is predicted to get worse over the next years [1,2]. According to a recent study, around 1.27 million annual deaths worldwide have been attributed to bacterial resistance in 2019, data that is expected to rinse to 10 million deaths by 2050 [3,4]. For that reason, AMR was recognized as a threat to the 2030 Agenda for Sustainable Development and in 2020 two new AMR indicators were included in the monitoring framework of the third SDGs "Good Health and Well-being". Furthermore, the World Health Organization (WHO) has stated that the pipeline of new antibacterial medicines is insufficient to tackle the challenge of increasing spread of antibiotic resistance. Altogether, it is evident that there is a constant need to keep improving the antibacterial armamentarium against multidrug-resistant (MDR) bacteria.

In this context, polymyxins, in particular polymyxin E (colistin) and polymyxin B, have been rescued as last resort antibiotics for the treatment of infections caused by MDR Gram-negative bacteria. Last-line therapeutic options include treatment of infections caused by carbapenem-resistant strains of *Acinetobacter baumannii*, *Klebsiella pneumoniae*, *Pseudomonas aeruginosa*, or *Escherichia coli.* In fact, polymyxins are considered a critically important antibiotic in human medicine by the WHO and its parenteral use is approved by the FDA as a salvage treatment of acute infections due to *P. aeruginosa*, *A. baumannii*, *Enterobacter* spp, *E. coli*, *Klebsiella* spp (particularly, *K. pneumoniae*) or *Citrobacter* spp resistant strains [5,6].

Despite its high activity against Gram-negative pathogens, polymyxins show significant adverse effects, particularly nephrotoxicity and neurotoxicity [7]. The major and well-known side effect of colistin administration is renal toxicity. However, it is widely reported in the literature that it also affects the nervous system in approximately 7 % of the cases, reaching 28 % after an intraventricular injection [8]. This neurotoxicity is mostly related to peripheral effects such as perioral paresthesia, dizziness, numbness of extremities, ataxia, vertigo, confusion, weakness, visual and speech disturbances, hallucinations, and seizures, probably due to the low penetration of colistin through the blood brain barrier (BBB) [9]. However, in specific scenarios such as the presence of sepsis or in those requiring repeated administration of colistin, there is a disruption of the BBB permeability, consequently increasing its brain uptake [10,11].

To date, the mechanism of colistin-induced toxicity remains unknown. However, it has been suggested that an impairment of the oxidant-antioxidant balance together with a mitochondrial dysfunction plays a key role [12,13]. Focusing on the CNS, numerous studies have shown that neurons, especially hippocampal neurons, are highly susceptible to oxidative stress. Thus, an imbalance in the antioxidant defenses could lead to synaptic alterations, inflammation, and neuronal death, which are considered the typical hallmarks of cognitive impairment and neurodegenerative diseases [14].

Although there are a few publications suggesting that colistin administration could lead to depression-like symptoms, behavioral abnormalities, and neuronal death in animal models, these studies are insufficient to understand the molecular mechanisms involved in colistin neurotoxicity [11]. Given the increasing need to use polymyxins to combat antibiotic resistance, it is crucial to gain a deeper understanding of their neurotoxicity at the molecular level. This knowledge will be essential for developing new strategies to prevent or reduce its toxicity. Thus, in the present work the molecular mechanisms involved in colistin-induced neurotoxicity were investigated through a combination of *in vivo* behavioral tests and *in vitro* and *in vivo* molecular studies.

2. Material and methods

2.1. Animals and treatments

6–8 weeks old C57BL/6 female mice (Envigo, Netherlands) were maintained at 22 ± 2 ºC and 60 % humidity with a 12 h light-dark cycle and *ad libitum* access to tap water and chow (Envigo, Madison, WI 53744–4220; 18 % protein and 6 % fat). To avoid depression-like behaviors related to the housing environment, animals from the same treatment were kept together in groups of 5. Following the human therapeutic approach animals were treated with an intraperitoneal (i.p.) injection of 9 mg/kg colistin or saline twice a day 8 h apart for 14 consecutive days. As previous studies showed that females are much more susceptible to polymyxin neurotoxicity than males [15], to simulate the worst-case scenario and better characterize polymyxin toxicity female mice were selected for this study. Body weight and food consumption were recorded every day. In order to calculate the food intake of each animal, the total food consumption of each cage was divided by the number of animals in the cage, assuming that all animals ate the same. 14 h after the last administration, four behavioral tests were performed on all animals. In all cases animals were given 10 minutes in the testing room before the start of the behavioral assessments to allow the animals to acclimate to the testing environment. Finally, mice were sacrificed 24 h after the last administration by cervical dislocation, or pentobarbital injection in those animals destined to obtain samples for immunohistochemistry.

Every effort was made to reduce the number of animals and minimize animal suffering. This procedure was approved by the Ethics Committee for Animal Experimentation of the University of Barcelona (CEEA) and accepted by the Department of Environment and Housing of the Generalitat de Catalunya with the license number 259/22.

2.2. Behavioral tests

2.2.1. Novel Object Recognition Test (NORT)

The recognition memory was studied by the NORT as described in Oliveira Da Cruz, et al. [16] with minor modifications. This test consists in two training days plus the day of the final test. Briefly, 48 h prior to the final test day, animals were set in a V maze area for 10 minutes without any object to explore the zone (habitation day). 24 h later, mice were placed in the same maze but this time 2 equal objects looking like a green plastic apple were located one in each arm of the V maze (training day). Finally, on the day of the test, one of the objects was replaced by a new one with similar size and same material but different color and shape. The time spent exploring each object was video recorded to posterior analysis. Results were expressed with the discrimination index (DI) following the equation (n = 6 animals/group):

$$DI = \frac{Novel\ Object\ exploration\ time - Old\ object\ exploration\ time}{Total\ exploration\ time}$$

2.2.2. Narrow beam test

To assess limb impairment an 80 cm wooden beam was placed horizontally 30 cm above a table with their home cage at the end of the beam [17]. One day before the test, 15 animals per group were trained to walk through the beam three times. The day of the test, mice were placed at the beginning of the beam and the number of foot slips, and the time needed to cross the whole beam was recorded.

2.2.3. Grid test

Animals were placed in a horizontal grid mesh measuring 25 cm height and 50 cm width. Then the mesh was turned upside down and the animals were video recorded for 1 minute. Afterwards the videos were analyzed blindly to determine the number of steps and immobility time [18] (n = 15 animals/group).

2.2.4. Forced Swimming Test (FST)

The forced swimming test was used to study the depression-like behavior of the animals [19]. Mice were placed into a 30 cm high, and 20 cm wide cylinder filled with water at 23 ± 2 ºC for 6 minutes. The immobility time during the last 4 minutes was recorded (n = 6 animals/group).

To ensure that the time elapsed since the last colistin injection was consistent across all animals, the behavioral tests were performed sequentially. The first test performed was the NORT, as it is the most likely to be influenced by stress. The Beam test was conducted in second place as it is a brief test requiring minimal physical exertion. Then, the Grid Walking Test was performed and, as it can be stressful and physically challenging, we let the mice rest for 30 minutes before continuing to the last test. After these 30 minutes, mice performed the Forced Swimming Test as it is the most physically demanding and most stressful.

2.3. Biodistribution study

LC-MS/MS was selected to quantify the amount of colistin in brain, kidney and liver as described in Kim K, et al. [20] with minor modifications.

2.3.1. Sample preparation

Brain, kidneys and liver of 3 animals per group were collected, weighted, and homogenized with milliQ water two times for 30 seconds using an electric homogenizer (Bel-art ProCulture, Fisher Scientific). Then, 10 μL of each sample were mixed with 120 μL of milliQ water and 15 μL Trichloroacetic acid 30 %. This was followed by a centrifugation of 5 minutes at 10,000 rpm and 4 ºC to precipitate proteins. Finally, the supernatant was collected and placed into liquid chromatography dark glass vials with insert (Agilent,)8010–0546) for further analysis. To quantify the amount of colistin, a calibration curve with the corresponding controls organs was carried out to avoid possible matrix effects.

2.3.2. Chromatographic conditions

Chromatographic analysis was carried out on a Triple Quad 6500 + LC-MS/MS system composed of a separation module (Chromatograph LC Agilent 1290 Infinity), an autosampler and solvent delivery system. Analytical separation of colistin was performed on a Tracer Excel 120 ODSB column (3 μM, 20 ×0.46 mm ID). The mobile phase was prepared with water: formic acid 0.5 % (A) and acetonitrile: formic acid 0.5 % (B) at the flow rate of 1.0 mL/min.

2.4. Evans blue assay

The integrity of the BBB was evaluated using the Evans Blue assay as described in Goldim M., et al. with some modifications in the mode of administration and dose [21,22]. Briefly, 14 h after the last administration of colistin, a 10 mL/kg of freshly prepared Evans blue solution was injected i.p. After 6 h mice were sacrificed by cervical dislocation and brains were removed, washed with phosphate-buffered saline (PBS) and frozen at –80 ºC for further analysis. The day of the analysis, brains were defrosted, weighted, and homogenized two times for 30 seconds using an electric homogenizer (Bel-art ProCulture, Fisher Scientific) with 3 mL of N, N-dimethylformamide. Samples were incubated for 24 h at 55 ºC, centrifuged 30 min at 15000 rcf and the colorimetric absorbance of the supernatant was measured at 620 nm using a microplate spectrophotometer (Benchmark plus, Bio Rad) (n = 3 mice per group).

2.5. Caspase-3 activity assay kit

To assess the apoptotic neuronal death, the caspase 3 activity was measured. Briefly, cortical tissue from 6 animals per group were homogenized according to manufacturer instructions (Abcam, Kit ab39383) and 200 μg of protein per well were placed in a 96 well plate. The fluorescence emission of the samples was measured with a fluorometer (Varioskan, Thermo Scientific) immediately after the addition of the reaction mixture and substrate at Ex/Em= 400/505 nm and again after 24 h incubation at 37ºC.

2.6. Hippocampal dendritic spines determination

To assess the number of dendritic spines in the hippocampus a minimum of 5 animals per group were sacrificed by cervical dislocation and brains were collected and processed following the instructions of the GolgiStainTM Kit purchased from FD Neurotechnologies, Inc. (FD Rapid GolgiStainTM Kit; Cat #PK401). Afterwards, brain sections of 100 μm of thickness were obtained using the cryostat (Leica Microsystems, Wetzlar, Germany) and those containing hippocampus were placed into slices for further staining. The quantification was carried out with Leica Thunder microscope (Leica Thunder Imager; Leica Microsystems) at 60x and z projection. A minimum of 5 images of the dendrites in Cornu Ammonis 1 (CA1) basal and apical, and Dentate Gyrus (GD) proximal and distal were taken of each animal (resulting in a total of 25 photos per area and group). To process and analyze the images, ImageJ v2.9.0/1.53t was used [23]. To make sure that spines from the same area were always counted, 20 μm from the end of the neuron or from the main branch were always left uncounted. Then, the following 30 μm were counted.

2.7. Primary neuronal cultures

This procedure was approved by the Ethics Committee for Animal Experimentation of the University of Barcelona (CEEA) with the license number OB119/20.

Two types of primary cultures were performed: pure hippocampal neuronal culture and cortical astrocyte-neuron mixed culture as described in Parcerisas A., et al. [24]. In both cases, brains from embryonic day 15–16 mice were dissected under a stereomicroscope with PBS-Glucose 3 %. The dissected cortex or hippocampus, without the meninges, were trypsinized (0.25 %) during 7 minutes at 37 ºC. To stop the digestion, horse serum in a 1:2 proportion was added together with DNAse (10 U/uL), and samples were incubated at 37 ºC for 7 more minutes. Then, the solutions were mechanically disaggregated by pipetting up and down 40 times. Afterward, the suspensions were centrifuged at 800 rcf for 6 minutes and the pellet was resuspended in supplemented Neurobasal medium containing 2 % B27, 1x Glutamax, 20 U/mL of penicillin/streptomycin supplemented with glial conditioned medium (2 % B27, 1x Glutamax, 20 U/mL of penicillin/streptomycin maintained in a glial confluence culture during 15 days) for pure neuronal culture or Neurobasal (0.5 mM glutamine, 0.02 % sodium bicarbonate, 45 % glucose, 20 U/mL of penicillin/streptomycin, 10 % horse serum and 2 % B27) for the mixed astroglia and neuronal culture.

Cells were counted with a Neubauer chamber and seeded in precoated plates with poli-D-lysine (0.05 mg/mL) at the desired concentration. Cells were incubated at 37 ºC and 5 % of CO_2.

2.8. MTT cytotoxicity assay

Cells of the mixt culture seeded at a concentration of 250 000 cells/mL were kept until DIV12. Then colistin at different concentrations (1000, 500, 250, 125, 62, 31, 16, 8, 4 μM) was added to the wells for 24 h. Subsequently, 6 μL of 2.5 mg/mL of MTT (3-[4,5-dimethylthiazol-2-yl]-2,5 diphenyl tetrazolium bromide) was added to the culture medium, including a background well, and kept during 1 h a 37 ºC and 5 % CO_2. Afterwards, the medium was removed, and the formazan crystals were dissolved with 100 mL of DMSO [25]. The absorbance of each well was measured at 565 nm with a microplate spectrophotometer (Benchmark plus, Bio Rad). For each colistin concentration, 3 wells were used as technical replicates in each of the 4 total independent

experiments.

2.9. Cell viability after Z-VAD-FM preexposure

To confirm the apoptotic effect of colistin, cells at DIV12 were pretreated with the caspase inhibitor Z-VAD-FM at 100 μM (Santa Cruz, sc-311561) for 1 h. Then, the medium was completely removed, and cells were exposed to different concentrations of colistin (1000, 500, 250, 125 μM) for 6 h. Finally, the viability of the cells was assessed by an MTT test in 3 independent experiments.

2.10. Flow cytometric analysis of Annexin V and PI staining

Cells at DIV12 were treated with colistin at a dose of 250 μM for 24 h. After this time, cells were washed with PBS, detached using 0.25 % trypsin and resuspended in PBS. Then, cells were incubated with 0.1 mg/mL of Annexin V-FITC (Sigma-Aldrich, APOAF) and 0.2 mg/mL of propidium iodide (PI) following manufacturer instructions for 10 minutes at room temperature (RT). Afterwards, the cell suspension was immediately analyzed using the cytometer Aria (Cell sorter: BD FACS Aria sorp) by triplicates.

2.11. Measurement of intracellular levels of ROS by DCFH-DA staining

The amount of ROS was measured with 2,7-dichlorofluorescein diacetate (DCFH-DA) fluorescent dye (Abcam ab113851) according to manufacturer instructions. Neurons at DIV12 were exposed to 250 μM of colistin for 24 h. Afterwards, cells were washed with PBS and 20 μM of DCFH-DA was added and incubated for 45 minutes at 37 ºC in the dark [26]. After this time, cells were washed with PBS and the DCFH-DA fluorescence was measured at Ex/Em = 485/535 nm with a fluorometer (Varioskan, Thermo Scientific) through 3 independent studies.

2.12. Evaluation of mitochondria membrane potential by JC-1 dye

Mitochondrial membrane potential is an indirect indicator of cell health and their apoptotic status. Thus, the mitochondrial membrane potential was studied using JC-1 - Mitochondrial Membrane Potential Assay Kit (Abcam ab113850). Cells at DIV12 were exposed for 24 h at 250 μM colistin. After treatment, cells were washed with PBS and incubated with 1 μM JC-1 dye for 10 minutes at 37 ºC and 5 % CO_2 in the dark. Afterwards, cells were washed with PBS and green (monomeric form) and red fluorescence (aggregate form) were measured with the fluorometer (Varioskan, Thermo Scientific) at Ex/Em: 488/535 and 535/590 nm respectively. A shift of fluorescence from red to green represents a loss of ψ_m. Thus, the ratios between fluorescence intensity in the red and green channels of 4 independent studies were calculated.

2.13. GFP transfection

To visualize dendritic spines, cells were transfected with GFP [27]. For that, pure neuronal cultures were transfected using a lentivirus (Cell Biolabs, LTV-300) expressing GFP. On the seeding day, 200 TU/mL of lentivirus were added to the culture medium for 6 h. After this time the medium was completely replaced, and neurons were kept until DIV21.

2.14. Immunofluorescence analysis

2.14.1. Brain sections

For immunohistochemistry, 24 h after the last administration mice were anesthetized with pentobarbital by an i.p. injection (100 mg/kg). When they were in the no-pain sleep phase, they were intracardially perfused with 4 % paraformaldehyde (PFA). After perfusion, brains were removed and stored 24 h at 4 ºC with PFA 4 %. Afterwards, the solution was replaced by PBS-30 % sucrose and left at 4 ºC a minimum of 48 h. After this time, brains were frozen and 20 μm coronal sections were obtained with the cryostat (Leica Microsystems, Wetzlar, Germany). Sections were stored at −20 ºC in a cryoprotectant solution (30 % distilled water, 30 % ethylene glycol, 30 % glycerol and 10 % phosphate buffer 0.1 M) until further use.

2.14.2. Cell culture

Transfected hippocampal neurons at DIV20 were treated with colistin at a dose of 64 μM for 24 h. Afterwards, cells were washed with 0.1 M PBS and fixed for 10 minutes with PFA 4 %. After this time, cells were rinsed 3 times with 0.1 M PBS until complete removement of the remaining PFA and stored with cryoprotectant solution at 4 ºC until further analysis.

2.14.3. Immunofluorescence

Selected brain slices or hippocampal fixed neurons were rinsed with PBS-1 % Triton. Then, they were incubated for 1 h with a blocking solution (10 % fetal bovine serum (FBS), 1 % Triton X-100, 0.2 % gelatin in PBS 0.1 M) at RT. Later, they were rinsed again with PBS-1 % triton and incubated overnight with the desired primary antibody. Next day, brain slices or hippocampal neurons were washed with PBS-1 % triton and incubated with the corresponding secondary antibody for 2 h at RT. Finally, they were washed with 0.1 M PBS and exposed to 0.1 mg/mL of Hoechst during 8 minutes for nuclei staining. Ultimately, samples were mounted in Superfrost microscope slides with Fluoromount-G™ medium and stored at 4 ºC. Images were obtained using Leica Thunder Microscope (Leica Thunder Imager; Leica Microsystems) and quantified by Fiji software [23]. In the case of brain sections, the quantification was carried out in the DG and in the CA1 and a minimum of 5 images per animal and 5 animals per group. For hippocampal neurons, a minimum of 20 neurons per group of 3 independent experiments were analyzed.

The following commercial primary antibodies were used for immunohistochemistry: anti-DCX (A8L1U, Cell Signaling, 1:500); anti-GFAP (Z0334, Dako, 1:1000); GFAP (17301, Synaptic Systems, 1:1000); anti-GFP (A11122, Invitrogen, 1:750); anti-IBA1 (O19–19741, Wako, 1:1000); anti-SOX2 (ab97959, Abcam, 1:500); and anti-Synaptophysin (106004, Synaptic Systems, 1:500). Alexa Fluor fluorescent secondary antibodies were from Invitrogen (A11011, A11001, A11075, A11008 and A32787)

2.15. Statistical analysis

All results are presented as the mean ± standard error of the mean (SEM). In all cases, Shapiro-Wilk normality test and a ROUT outlier test were performed. If data followed a normal distribution, a double-sided group T-test between two groups was performed. In the MTT assay, as we were comparing different concentrations a one-way ANOVA or two-way ANOVA in the case of Z-VAD-FM exposure were performed. In both cases, these analyses were followed by Bonferroni's post-hoc test. When data followed a non-parametric-distribution, Mann-Whitney-U-test was performed to compare two groups. All analyses were obtained using Graph Pad Prism version 8.2.1 (Graph Pad Software, Inc.).

3. Results

3.1. Colistin alters body weight gain, nephrophysiology, and peripheral nervous system

The *in vivo* conditions established to analyze the effects of colistin were evaluated. To this end, nephrotoxicity and disruption of the peripheral nervous system (PNS) (locomotion and strength) were determined, as they are considered the main side effects of colistin treatment. Thus, 7 weeks-old female mice were administered i.p. with 9 mg/kg colistin 8 h apart for 14 days (Fig. 1a).

First, to assess general toxicity parameters, the body weight and food intake were measured. Our study demonstrated that colistin caused a significant decrease ($p < 0.0001$) of body weight (Fig. 1b), while no

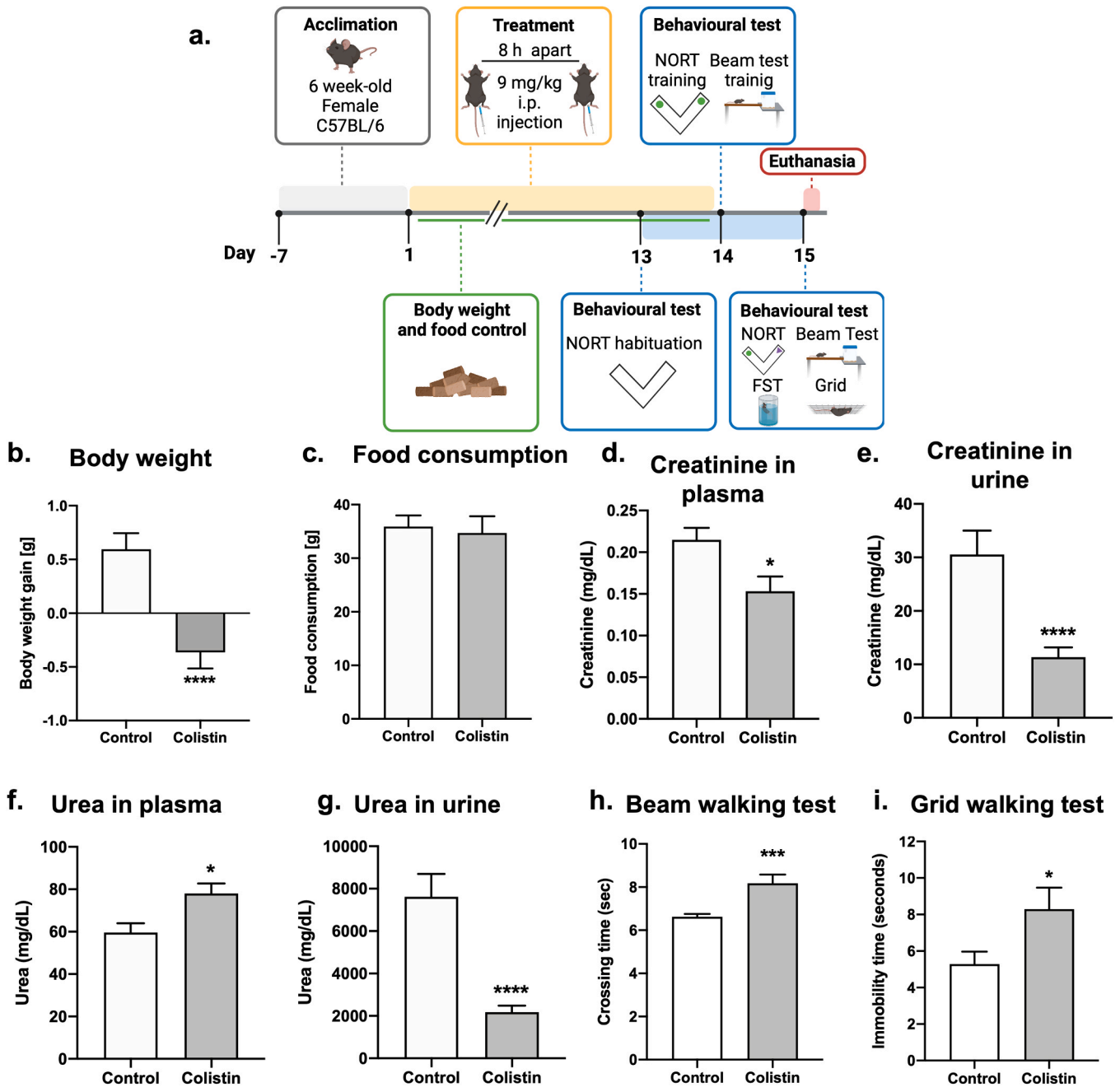

Fig. 1. Evaluation of general toxicity parameters, nephrotoxicity and alterations in the PNS in colistin treated mice. (a) Graphical summary of the methodological procedure. (b) Body weight gain after 14 days of treatment. (c) Accumulated food consumption. (d-e) Creatinine concentration found in plasma and urine, respectively. (f-g) Urea concentration found in plasma and urine respectively. (h) Seconds spent crossing the beam (i) Immobility time in the grid. In all cases results are expressed as the mean of 15 animals ± SEM. Statistical analysis was conducted through Mann-Whitey-U- test. In all cases, * $p < 0.05$, * * $p < 0.01$, * ** $p < 0.001$ and * ** * $p < 0.0001$. Fig. 1(a) was Created in BioRender. Guzman, L. (2025) https://BioRender.com/v81y211.

significant differences were found in food intake (Fig. 1c). Regarding the nephrotoxicity, the levels of creatinine and urea in plasma and urine were evaluated. Interestingly, colistin caused a global decrease of creatinine levels in both fluids while for urea a significant increase ($p = 0.0453$) in plasma and a significant decrease ($p < 0.0001$) in urine (Fig. 1d-g) were found. To confirm the effects in locomotion and strength, the beam and grid walking test were performed. Colistin treated mice showed a significant increase ($p = 0.0005$) in the beam crossing time compared to control (Fig. 1h). Moreover, they also showed a significant increase ($p = 0.0355$) of the immobility time in the grid walking test (Fig. 1i).

3.2. Colistin reached the brain by altering the blood brain barrier

To assess whether colistin was able to reach the brain and its distribution in the main organs involved in its pharmacokinetics, a biodistribution study measuring colistin levels in brain, liver and kidneys was conducted. Our results showed that after a 14-days treatment, colistin was especially accumulated in kidneys (1351.47 ± 218.99 mg/kg) and in second place in liver (24.44 ± 6.88 mg/kg) (Fig. 2a). Although at low concentration, colistin was also detected in brain tissue at a concentration of 0.5 ± 0.09 mg/kg (Fig. 2a). Due to its molecular structure, colistin is not expected to cross the BBB [28] so, to understand why colistin is reaching the brain, the integrity of the BBB was

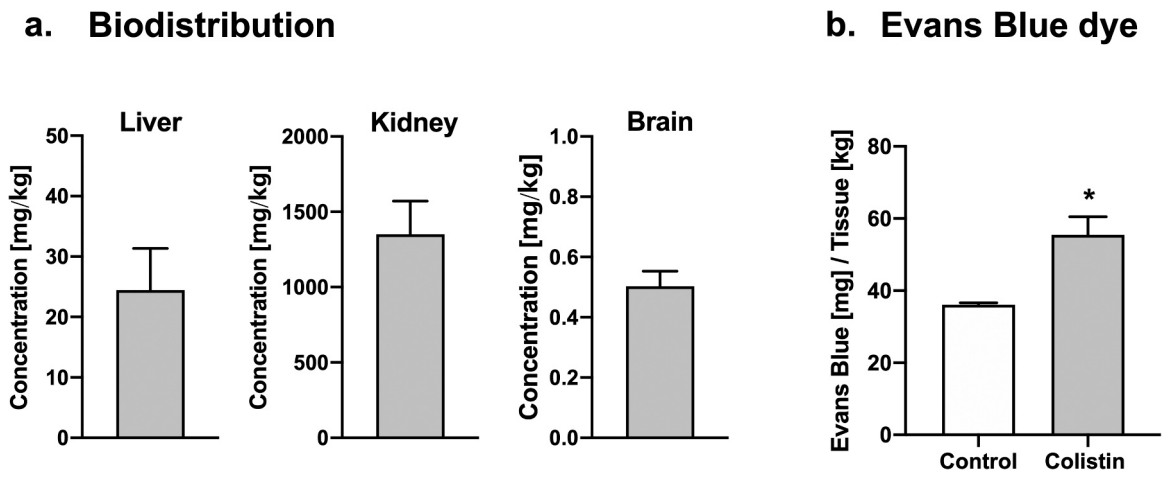

Fig. 2. Biodistribution of colistin and BBB integrity evaluation. (a) The concentration of colistin found in the liver, kidney, and brain after 14 days of colistin treatment. Please note the Y scale changes between organs. **(b)** Amount of Evans blue found in brain homogenate. Results are expressed as the mean ± SEM with 3 animals per group. Statistical comparison for Evans blue quantification was conducted through a group two-tail T-test, * indicating a p-value< 0.05.

examined. Injections of Evans blue in colistin-treated and untreated mice showed a significant increase ($p = 0.0181$) of this dye in colistin-treated mice brains compared to controls, suggesting that a 14-days of colistin treatment promoted an alteration of the BBB (Fig. 2b).

3.3. Colistin induces neuronal cytotoxicity by activating an apoptotic pathway

To study the neuronal cytotoxic effects of colistin, a first *in vitro* approach using a primary mixed cortical culture was performed. Neurons at DIV12 were treated with different concentrations of colistin for 24 h. Colistin induced a concentration-dependent decrease in cell viability compared to control, a no observed adverse effect level (NOAEL) of 8 μM and a LC_{50} of 222 μM with a 95 % CI of 174.3–285.8 μM (Fig. 3a).

To further investigate the cytotoxic effects of colistin, cells were treated for 24 h with 250 μM (the concentration tested more similar to the calculated LC_{50}) and exposed to 0.1 μg/mL of Annexin V and 0.3 μg/mL of PI for 10 minutes. The percentage of cells in the early apoptotic

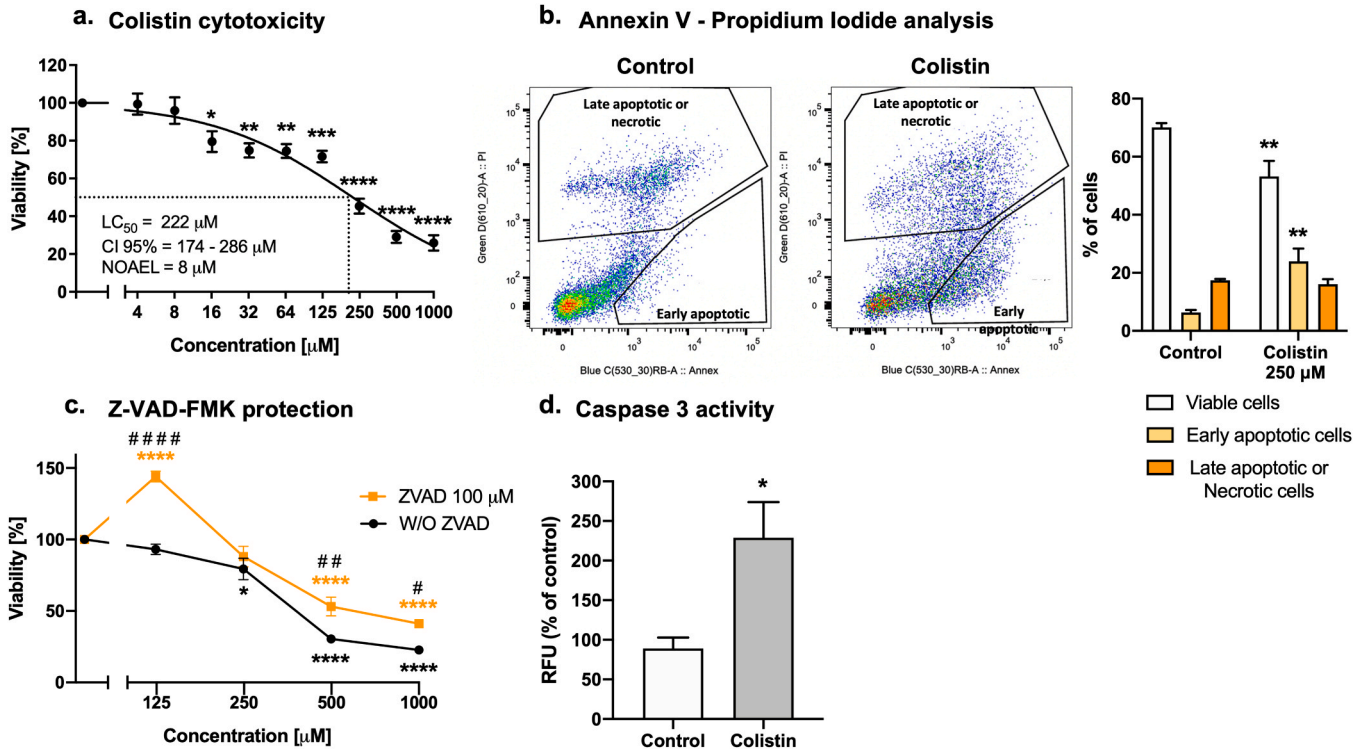

Fig. 3. Evaluation of the molecular pathway of colistin induced cytotoxicity in primary cortical neurons. (a) Changes in cell viability of mixed astrocyte-neuron culture after 24 h treatment with different concentrations of colistin. (b) Flow cytometer analysis of Annexin V – PI staining of 250 μM colistin treated cells. (c) Viability of 1 h pre-exposed neurons with 100 μM Z-VAD-FMK compared to neurons not exposed to Z-VAD-FMK. (d) Increase of caspase-3 activity in mice cortical tissue. All results are expressed as mean ± SEM in % of control (and a minimum of 3 independent experiments were done). Statistical comparisons were performed by one-way (a) or two-way (b, c) ANOVA with Bonferroni's post-hoc test or group two-tail *t*-test (d). * Indicates significant differences with the control. # Indicates significant differences between points at the same concentration of colistin. * p-value < 0.05, * * p < 0.01, * ** p < 0.001 and * *** * p < 0.0001.

stage (Annexin V positive cells) or late apoptosis/necrosis (PI + Annexin V) were evaluated by flow cytometry. As expected, colistin treated cells show a significant decrease of viable cells ($p = 0.0059$). The early apoptotic cells increased from 8.1 % in the control group to 32.5 % with colistin ($p = 0.0043$). No significant differences were seen in late apoptotic or necrotic cells (Fig. 3b).

As a complementary approach to confirm the cellular death pathway and the implication of caspases in colistin induced cytotoxicity, the neuronal culture was pre-exposed to the pan caspase inhibitor Z-VAD-FMK. Pre-exposed mixed culture significantly increased the viability of the culture at colistin concentrations of 125, 500 and 1000 μM ($p < 0.0001$; $p = 0.0072$ and $p = 0.0345$ respectively) (Fig. 3c).

As a cell culture does not represent completely the complexity of an *in vivo* model, the effects of colistin on neuronal apoptosis through caspase activation were evaluated in the cortical tissue of C57BL/6 mice model. *In vivo* results, in accordance with *in vitro* results, revealed a significant increase ($p = 0.0142$) of caspase-3 activity in colistin-treated mice (Fig. 3d).

3.4. Colistin causes an increase of ROS levels and mitochondrial dysfunction in cortical neurons

With the aim to investigate the underlying mechanisms that lead colistin to induce neuronal apoptosis, several important hallmarks related to oxidative stress and inflammation were studied. Firstly, ROS levels and mitochondrial membrane potential were evaluated in primary cortical cultures exposed to colistin. After 24 h of colistin treatment (250 μM) the intracellular ROS levels increased to 270 % compared to control ($p = 0.0175$) (Fig. 4a). Moreover, a mitochondrial dysfunction was detected, seen as a decrease of the ratio aggregate/monomeric forms (34 % decrease, $p = 0.0451$) which reflects a loss of membrane potential (ψm) (Fig. 4b).

3.5. Colistin causes an increase of astrogliosis but not microgliosis

Neuroinflammation plays an essential role in pathological features associated with a wide variety of diseases. For that reason, the effect of colistin in glial reactivity was analyzed in colistin-treated mice. Astrocytic and microglial reactivity was evaluated in different hippocampal areas (DG and CA1) by detecting glial fibrillary acidic protein (GFAP) for astrogliosis and ionized calcium binding adapter molecule 1 (IBA1), for microgliosis. Our results showed a significant increase of GFAP fluorescence in DG and CA1 ($p = 0.009$; $p = 0.022$, respectively) of colistin treated mice, together with more reactivity seen through morphology changes, in comparison to control mice (Fig. 5a,b,e). However, no significant changes in intensity or morphology were seen in microglial cells, detected with anti-IBA1 protein, in DG nor CA1 ($p = 0.404$; $p = 0.997$) (Fig. 5c,d,e).

3.6. Colistin decreases dendritic spines in granular hippocampal neurons

As the neuronal loss and an increase of oxidative stress have been described to be straightly related to cognitive impairment, we evaluated the effects of a 14-days colistin treatment in cognition and depression. For that, the NORT and the FST were performed. Our results indicate that colistin-treated mice presented a significant decrease of the discrimination index in the NORT compared to their control littermates ($p = 0.0008$), clearly indicating that colistin caused a memory deficit (Fig. 6a).

To ensure these results were specific of cognitive impairment and were not biased by motor dysfunction, the total time each animal spent exploring both objects, as well as the time spent on each one, was evaluated on the training day (Suppl. Fig. 1).

On the other hand, regarding the effects in the FST, colistin-treated mice showed an increase of the immobility time compared to controls ($p = 0.0071$), indicating that colistin also causes depression-like symptoms in mice (Fig. 6b).

As another important hallmark of cognitive decline is dendritic spine loss, the number of spines of hippocampal neurons was also analyzed. The number of dendritic spines in the proximal area of the DG of colistin treated mice decreased from 84.35 ± 10.62–55.12 ± 3.49 ($p = 0.0234$). Moreover, colistin also caused a significant decrease ($p = 0.0128$) of the spines found in the distal area of the DG (Fig. 6c). However, no differences were seen in the CA1 neither apical nor basal zone (Fig. 6d).

3.7. Colistin causes a decrease of the postsynaptic protein PSD95

To determine if colistin affects not only the total number of dendritic spines, but also the synaptic signaling, hippocampal neurons were transfected with GFP in order to label all the neuronal projections. Then,

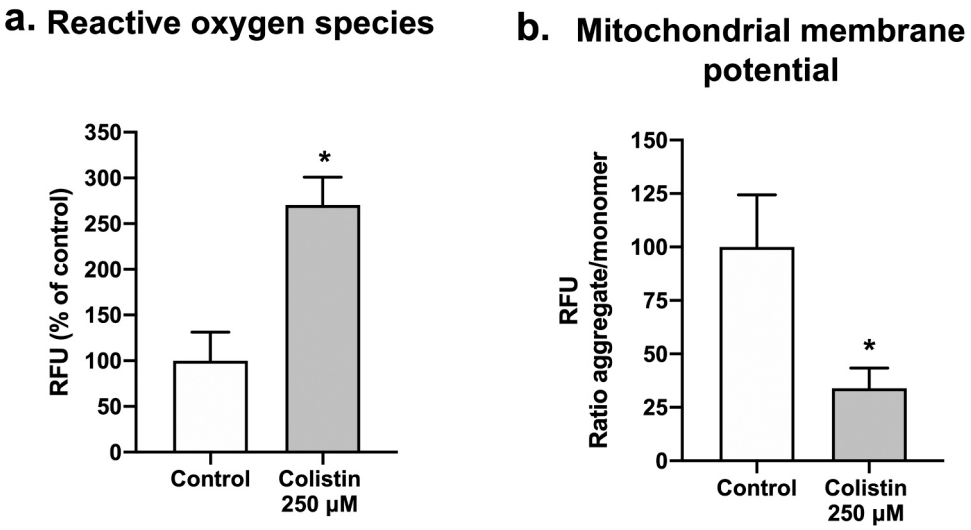

Fig. 4. Assessment of ROS and mitochondria membrane potential in primary cortical neurons. Cells were treated at DIV12 with 250 μM of colistin during 24 h. (a) Representative images of DCFH-DA staining and its quantification with the fluorimeter. (b) Quantitative analysis of cationic fluorescent indicator JC-1 in 250 μM colistin treated cells. Data are presented as the ratio between JC-1 aggregate form (high membrane potential) and the monomer form (low membrane potential). Results are expressed as mean ± SEM in % of control (and a minimum of 3 independent experiments were done). Statistical analysis was performed with a two-tail group *t*-test. * Indicates significant differences with the control (p-value < 0.05).

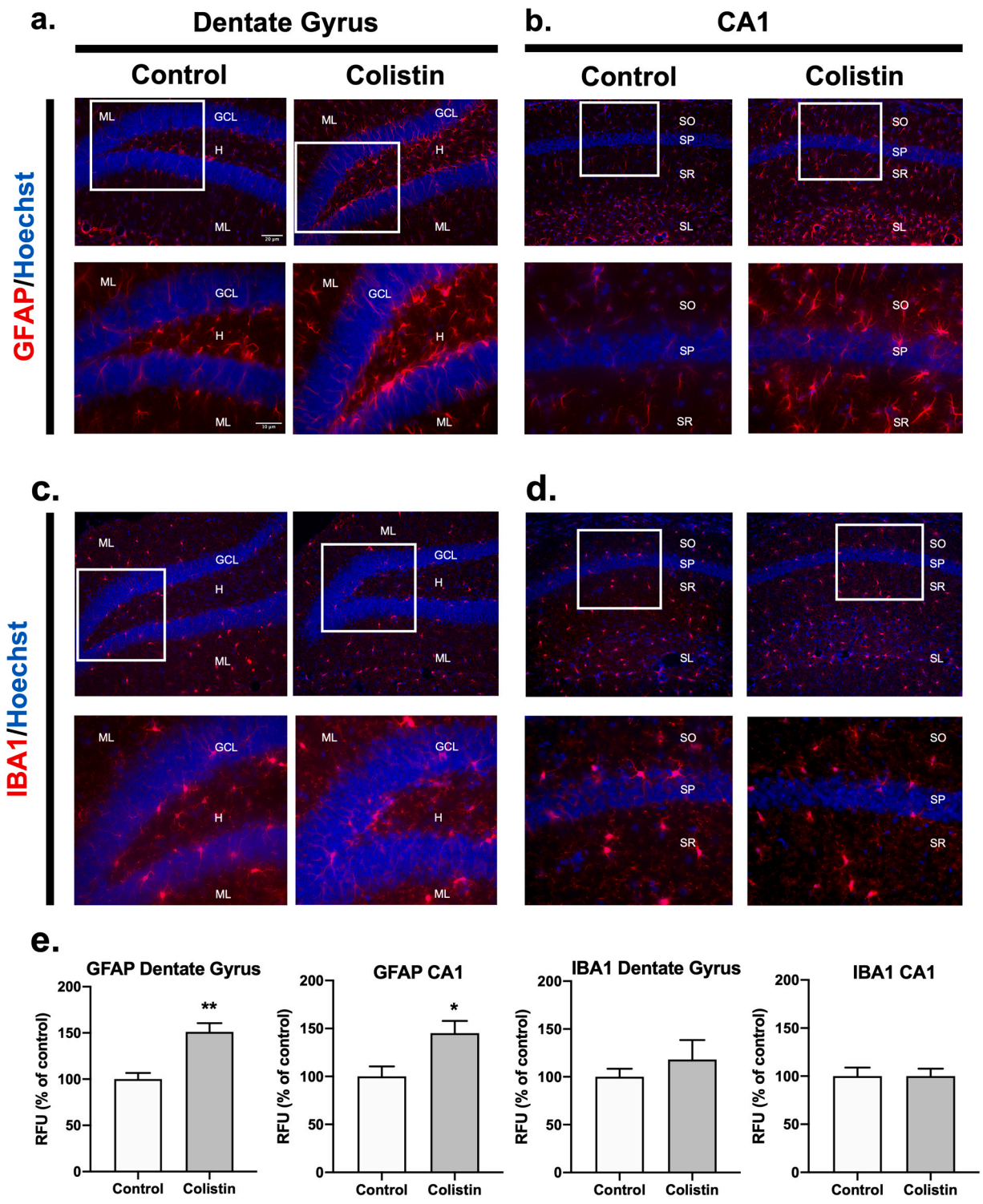

Fig. 5. Evaluation of inflammatory responses. Representative image of immunohistochemistry against GFAP of control and colistin-treated mice in DG (a) and CA1 (b). Representative image of immunohistochemistry against IBA1 of control and colistin-treated mice in DG (c) and CA1 (d). (e) Graphical representation of the fluorescence intensity of GFAP and IBA1 in DG and CA1. Images were taken at x20 and x40 magnification. Fluorescence quantification was measured as the mean intensity divided by the area of DG or CA1. Results are expressed as the mean ± SEM in percentage of the control. A minimum of 5 animals per group and 5 images per area (DG and CA1) and animals were analyzed. Statistical analysis was performed using a group two-tail T-test. * p-value < 0.05, * * $p < 0.01$. ML: Molecular layer, GCL: Granule Cell Layer, H: Hilus, SO: Stratum Oriens, SP: Stratum Pyramidale, SR: Stratum Radiatum.

the distribution pattern of synaptophysin (a presynaptic protein) and PSD95 (a postsynaptic protein) were analyzed. To ensure that the observed effects were specific to synapsis and not due to lethality, cells were treated at DIV20 with a colistin concentration that did not cause any cytotoxicity (64 μM) (Suppl. 1).

The results reported with hippocampal neurons transfected with GFP, supported that colistin caused a significant reduction of the total number of dendritic spines ($p = 0.01$), thus in accordance with the *in vivo* results. Related to the synaptic proteins, when normalized with the number of spines, no differences were seen in synaptophysin. However,

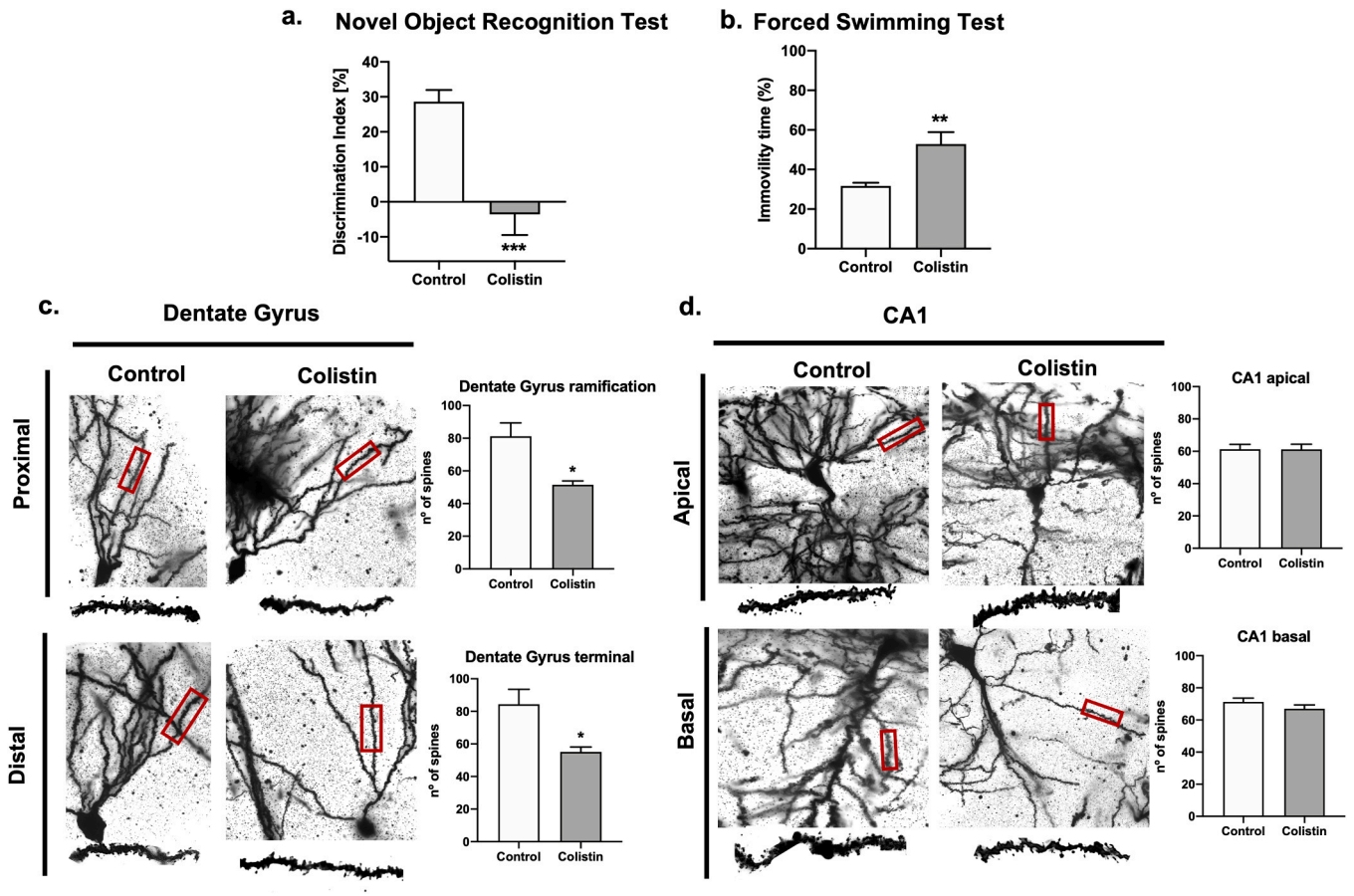

Fig. 6. Evaluation of cognitive function and depression-like behavior through behavioral tests and dendritic spines. (a) NORT analysis represented as the DI (n = 6). (b) FST represented with the immobility time in % of control (n = 6). (c) Representative optical microscope images of DG in terminal and ramification area of control and colistin treated mice. Quantification of dendritic spines of each 30 μm of dendrite in both areas. (d) Representative optical microscope images of CA1 in apical and basal areas of control and colistin treated mice. Quantification of dendritic spines of each 30 μm of dendrite in both areas. A minimum of 4 animals per group and 5 different neurons per animal were analyzed. Statistical analyses were performed with a group two-tail *t*-test. * Indicates significant differences with the control (p-value < 0.05).

PSD95 positive spines were significantly reduced by 25 % ($p = 0.088$) in colistin-treated cultures. Consequently, a significant reduction of the colocalization of the three proteins was also observed (Fig. 7a,b).

3.8. Colistin treatment alters adult neurogenesis by decreasing the number of DCX positive neurons

As the main effects of colistin were identified on the DG neurons, and the hippocampal adult neurogenesis is a specific process that plays a crucial role in preserving cognitive function in this region [29], we studied the effects of colistin in different stages of the neurogenic process. With that purpose, an immunohistochemistry against SOX2, GFAP and DCX proteins were performed. SOX2 is a protein expressed in early neural precursor cells that, combined with a co-expression with GFAP, indicates the total number of stem cells in the subgranular layer. On the other hand, DCX is a marker for immature neuronal cells.

Our results showed that colistin did not alter the number of SOX2 or SOX2-GFAP positive precursors (p value> 0.1 in all cases) (Fig. 8a). However, it significantly decreased the number of DCX positive cells located in the subgranular zone (SGZ) and granular layer (GL) of the DG ($p = 0.098$; $p = 0.036$) (Fig. 8b).

4. Discussion

The massive increase in AMR has made necessary the reintroduction of antibiotics that are effective but have a narrow therapeutic window, like colistin. Although poorly understood, neurotoxicity is the second major side effect of polymyxin therapy [15]. However, the actual studies of neurotoxicity are mainly focused on the PNS, while little attention has been paid to the CNS toxicity. Interestingly, the main results of this study revealed that colistin affected the CNS in different ways, such as inducing astrogliosis and neuronal death by the activation of caspase 3. Thus, lead in turn to depression-like symptoms, and cognitive impairment. Moreover, and to the best of our knowledge, this study has demonstrated, for the first time, that colistin reduced the number of dendritic spines, compromising synaptic function.

In this study, it was found that 14 days 18 mg/kg/day colistin treatment provokes a significant loss in body weight, whereas no differences in food consumption were found. This weight loss could be an indicator of nephrotoxicity since it has been demonstrated that impairment of renal function produces an increase in muscle wasting, which is directly related to muscle atrophy [30]. To determinate if this colistin treatment cause renal dysfunction, the levels of creatinine in plasma and urine were evaluated. An increase in the ratio plasma: urine is a widely known as a measure for kidney injury [31]. Besides, creatinine is also involved in other molecular processes like intramuscular metabolism [30,32]. In this study colistin-treated mice showed a decrease of creatinine levels in both urine and plasma. This discrepancy observed in the results suggests that since mice demonstrated muscle alterations by a decrease of the body weight and strength, in line with previous studies [33–35] creatinine levels would not be considered an appropriate parameter to determine kidney function.

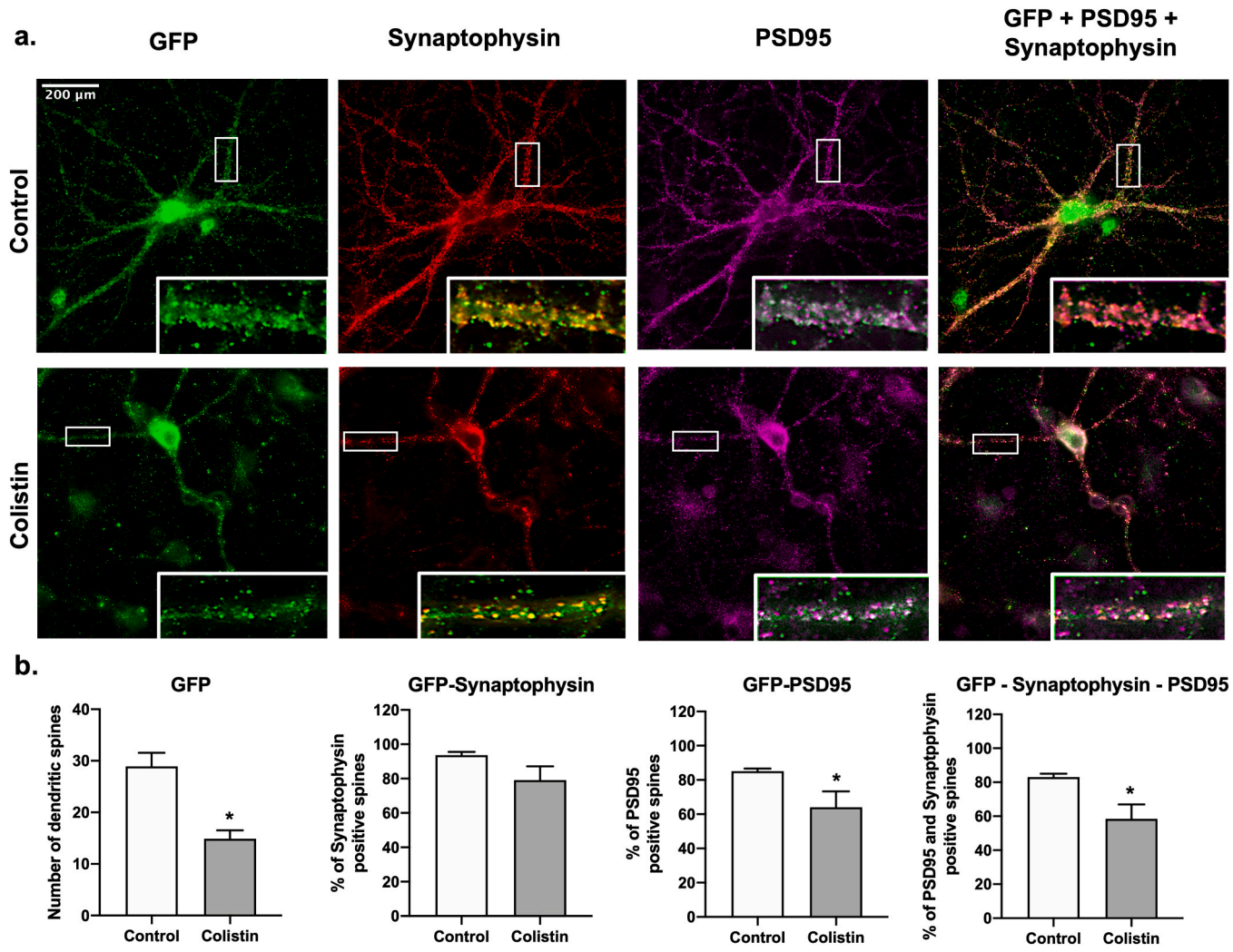

Fig. 7. Evaluation of dendritic spines and synaptic proteins. (a) Representative images for the detection of GFP, Synaptophysin and PSD95. Graphical representation of the number of dendritic spines for GFP (b), GFP colocalized with Synaptophysin (c) or PSD95 (d) and both (e). In all cases statistical analysis was performed with group two tail T-test (n = 3). * Indicates $p < 0.05$ compared to control.

Supporting these data, it has been well described that muscle weakness is one of the main clinical adverse effects of colistin [36,37]. This may be caused by a blockage in the release of acetylcholine to the synaptic gap affecting the neuromuscular junction and therefore reducing muscle contractility, which may lead to muscular atrophy. To assess if this therapeutic regimen caused signs of muscular weakness, the Grid test was performed [38,39]. This test measures fore- and hindlimb muscle strength as an inducer of neuromuscular function. In accordance with the previous results, it was observed that colistin caused muscle weakness in mice [40–42]. Therefore, to study the nephrotoxicity, as it was seen that creatinine was not a good endpoint to assess the renal function, the urea levels in urine and plasma were evaluated. In this case, in accordance with clinical practice, colistin treatment caused a decrease of urea in urine and an increase in plasma, indicating an impairment of the renal function.

Regarding neurotoxicity, the reported adverse effects of colistin treatment in humans included confusion, dizziness, paresthesia, visual disturbances, and ataxia, among others. Thus, to detect deficits on balance and motor skills, the beam test was performed [43,44]. In accordance with clinical data and *in vivo* studies in multiple animal models, the results of this study indicated that colistin-treated mice showed locomotion alterations [45–49]. All these results together indicate that an i.p. colistin administration of 18 mg/kg/day for 14-days is a good model to study the effects on the CNS, therefore validating this study design. Moreover, the dose selected fits within the low range of human clinical doses, when the allometric interspecies dose conversion is applied [50].

Colistin's ability to reach the brain is a subject of ongoing debate. Its physicochemical properties, including its high molecular weight, hydrophilicity, and cationic charges, hinder its passage across the BBB [51,52]. Supporting this, studies have shown that seven days of colistin treatment with a daily injection at a dose of 7 mg/kg, does not alter the BBB and is not detectable in the brain [53,54]. In contrast, some authors have suggested a possible increase in BBB permeability caused by continuous administration of colistin and by a systemic infection, which could compromise BBB integrity, leading to the enhancement of drug entry into the brain [55]. In this study, it was demonstrated that after 14-days of colistin administration at a dose of 9 mg/kg twice a day, low concentrations of this drug were able to reach the brain. Moreover, it has been observed that animals treated with colistin showed an increase in the amount of Evans blue in the brain, indicating an alteration of the BBB permeability and probably allowing colistin to enter the brain.

In this sense, colistin is known to increase the ROS levels and the nervous system is particularly sensitive to oxidative stress due to the high levels of polyunsaturated fatty acids and high oxygen consumption. An imbalance in the antioxidant defenses can lead to altered neuronal signaling, neuroinflammation, and activation of cell death mechanisms [56–59]. Additionally, it is known that an excessive accumulation of

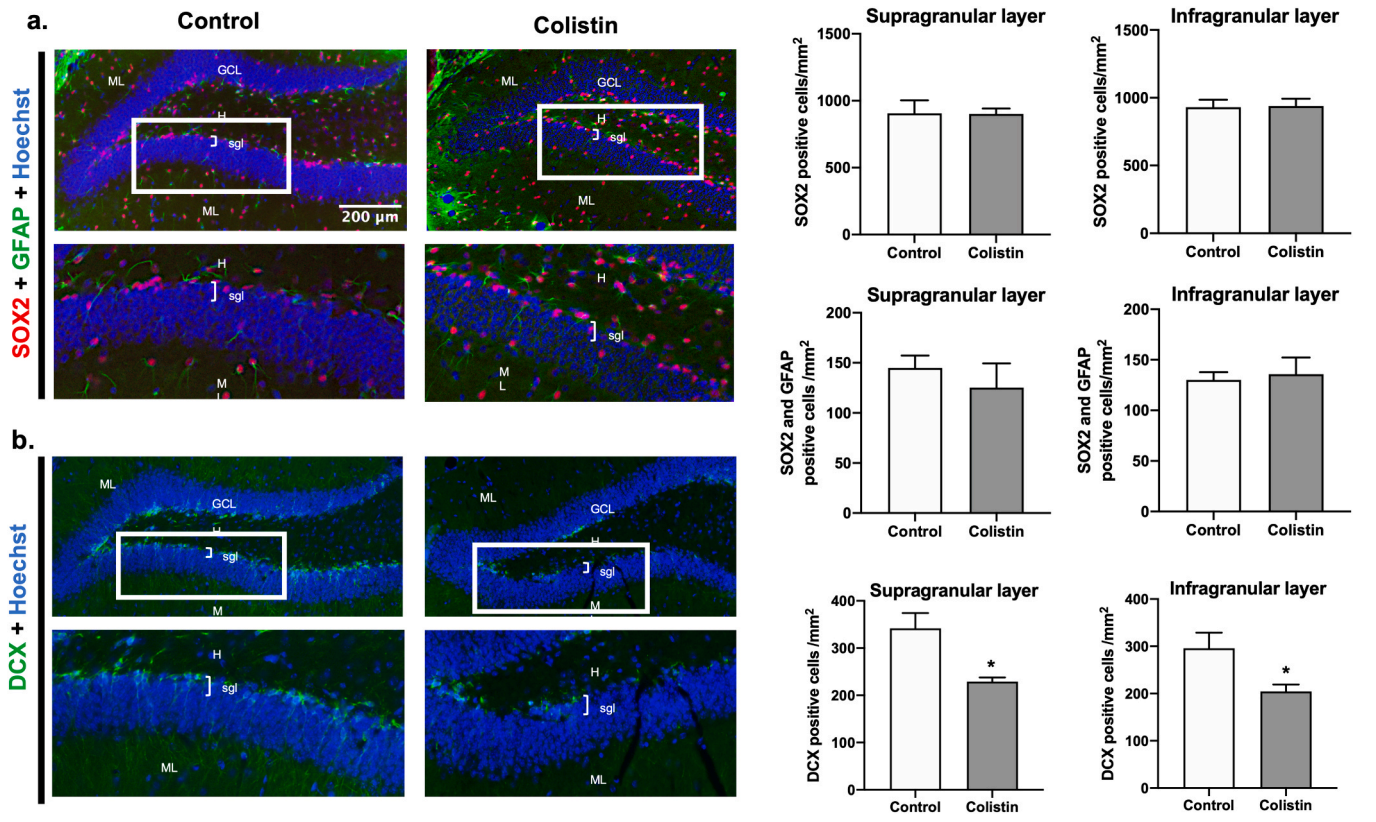

Fig. 8. Evaluation of colistin effects in neural stem cells and immature neuronal cells. (a) Representative images of the immunohistochemistry against SOX2-GFAP and DCX in control and colistin-treated mice. (b) Quantitative analysis of SOX2, SOX2-GFAP or DCX positive neurons in the supragranular and infragranular layer of the DG. In all cases statistical analysis was performed with group two tail T-test (n = 3). * Indicates $p < 0.05$ compared to control. ML: Molecular layer, GCL: Granule Cell Layer, H: Hilus, SGL: Subgranular layer.

ROS is closely linked to mitochondrial dysfunction, which ultimately activates the caspase-3 pathway and leads to apoptosis [60,61]. In this line, co-cultures of cortical primary neurons and astrocytes were used to establish a more physiologically relevant model to assess colistin toxicity in detail. Consistent with other studies [62], these results showed that colistin increased oxidative stress, causing mitochondrial membrane potential dysfunction, a general indicator of mitochondrial health. Moreover, the findings of this study demonstrated that colistin induces apoptotic cell death, as indicated by an increase in Annexin V staining. Corroborating this result, a partial protection when cultures were pre-exposed to ZVAD-FMK, a pan-caspase inhibitor were observed. However, the lack of total protection suggests that not all cell death is caspase dependent. Therefore, other mechanisms may be involved in colistin toxicity.

Related to neuroinflammation, an astrogliosis induction was observed in DG and CA1 of colistin treated mice, in accordance with previous studies in which colistin increased GFAP levels, a type of intermediate filament found in astrocytes [63,64]. Astrocytes are involved in the inflammatory process but also participate in BBB homeostasis [65,66]. This astrocytic capacity together with the no effect detected on microglial cells, critical regulators of the inflammatory process, suggest that the observed astrogliosis after colistin administration may be related to alterations in the BBB more than to inflammatory processes. Moreover, the induced astrogliosis could be also associated with excitatory effects since it has been evidenced that colistin causes an impairment in glutamate and calcium levels leading to long-term depression (LTD) and excitotoxicity [67].

Neural plasticity, including synaptic plasticity and neurogenesis, is the ability of the nervous system to modify itself in response to a stimulus. Thus, a correct function of synapse and adult neurogenesis is essential for a correct working memory, especially in the hippocampus. When ROS accumulation occurs in this area, it leads to memory loss and cognitive deficit [68–70]. In fact, both glial activation and ROS increase are known to play a critical role in neurodegenerative diseases characterized by cognitive decline. Consistent with this, the results of this study demonstrated that animals treated with colistin showed memory loss in the NORT, a test used in animals to study short- and long-term recognition memory. Moreover, FST results revealed that colistin also induced depression-related effects. In this context, although various studies have demonstrated a strong relationship between ROS accumulation, and the early onset of dementia [71,72], to the best of our knowledge, little is known about the connection between colistin treatment and neurodegeneration has not been studied.

In this study it has been clearly demonstrated the neurotoxicity induced by colistin *in vivo* and *in vitro*, and it has been proven that colistin reaches the brain. However, the concentration detected in brain after 14 days of administration (0.5 mg/kg) corresponds approximately to 0.4 µM, which is 40 times lower or more than the concentrations inducing adverse effects in the *in vitro* studies (16 µM for neuronal cell death, 64 µM for reduction in dendritic spines, 250 µM for ROS). Possible explanations for this discrepancy are, among others, that the concentration detected in brain was obtained from a whole brain homogenate and cannot exclude that in one or the other area higher concentrations have been achieved. It could also be explained by the extensive loss of colistin *in vitro* due to its high adherence to plastic [73] which would mean that the real concentration reaching cells in culture could be much lower than the concentration added to the medium. However, another potential explanation arises considering the nephrotoxicity of the compound, because acute kidney injury is often accompanied by uremic encephalopathy [74]. This is the possibility that the CNS neurotoxicity observed could be indirectly induced by colistin opening the BBB and creating a pharmacokinetic alteration in the

distribution of uremic toxins. That is to say, that colistin could be allowing that the organic waste caused and accumulated by renal disfunction reaches the CNS and thus causes a uremic encephalopathy status in the animals. This unexplored hypothesis is supported by the fact that the behavioral symptoms of colistin treated animals highly match to the ones caused by indoxyl sulfate, one of the most potent uremic toxins (apathetic behavior, reduced locomotor and reduced exploratory activity) [75–77]. Also, by studies showing that indoxyl sulfate has direct neurotoxic actions like neuronal death and astrocyte activation, it increases the production of ROS and decreases markers of neurogenesis, including doublecortin [78,79]. If colistin neurotoxicity *in vivo* is induced by direct or indirect effects will need further investigation in future studies, but colistin has for sure a direct neurotoxic potential proved *in vitro* and it is nephrotoxic *in vivo*, so it is therefore important to discuss its effects with a comprehensive *in vitro-in vivo* extrapolation perspective.

In general terms, neurotoxicity of antibiotics is well-documented. Aminoglycosides (peripheral neuropathy, encephalopathy), cephalosporins (reversible encephalopathy with temporo-spatial disorientation and triphasic waves on EEG), penicillin (encephalopathy, behavioral changes, myoclonus, seizures) and quinolones (seizures, confusion/encephalopathy, myoclonus, and toxic psychosis) are some among other members of this family of drugs that present potential neurotoxic adverse effects [80]. Hence, appropriate dosage and monitoring of the patient at medical level is compulsory not only to prevent AMR spreading but to prevent toxicity side effects. However, the onset of dementia is difficult to detect because it is not immediately apparent, and long-term follow-up and specific cognitive tests are required. Nonetheless, given the extensive evidence regarding neuronal death, astroglia activation, and cognitive impairment following colistin treatment, we believe that it is essential to conduct a retrospective study to evaluate the relationship between colistin treatment and the onset of cognitive decline.

It has been demonstrated that dendritic spine loss directly correlates with loss of synaptic function [81–83]. Depending on the affected part of the brain, different symptoms may arise. To understand the effects of colistin on memory, the CA1 and DG regions of the hippocampus were examined [84]. These two sections are part of the tri-synaptic circuit (entorhinal cortex layer II - DG - CA3 - CA1), which is essential for memory formation and spatial orientation. Surprisingly, after colistin treatment, only dendritic spines of neurons in the DG were affected, but not those in the CA1. Although both areas have a very similar laminar structure, they differ in the density and distribution of various receptors and ion channels, which could be responsible for the different responses to drugs [85]. This regional specificity could imply varying vulnerabilities within hippocampal substructures to colistin exposure, although more studies need to be done in order to understand the specific underlying mechanisms.

Various types of dendritic spines with different morphologies have been described. Filopodia (thinner and longer) are immature spines lacking synaptic function, whereas mushroom are mature spines [86–88]. Therefore, to study the synaptic function, it is essential to assess not only the total number of spines but also their type. Since identifying spine types based on morphology can lead to misclassification due to its difficulty, the evaluation of pre- and post-synaptic proteins like synaptophysin and PSD95 was performed in primary neuronal cultures to identify functional spines. This model, unlike most cell lines, is able to generate spines and new synapses, allowing the determination of the effect of colistin in synapsis modulation.

Synaptophysin is considered one of the best markers for studying synaptic density [89,90]. It is found in the presynaptic nerve terminals and is necessary for the formation of new synaptic vesicles. In contrast, PSD95 is located at the postsynaptic membrane and interacts with other synaptic proteins, which are necessary for the formation and maintenance of excitatory synapses [91]. The results of this study demonstrated that low concentrations of colistin, where neuronal death has not yet occurred, not only causes a reduction in the number of spines but also affects the PSD95 levels of the remaining spines. In this context, it has been reported that a reduction in PSD95 leads to a loss of AMPA receptors correlated with defective LTD activity, a process that is involved together with long-term potentiation (LTP) in information storage and memory consolidation [92,93]. This alteration would explain the cognitive impairment observed after colistin treatment [94].

The DG is one of the few areas of the mouse brain where neurogenesis has been detected during adulthood. The hippocampal neurogenic niche is located in the subgranular zone of DG, which is primarily composed of neural stem cells (NSCs). These cells are divided and generate neuronal progenitors that are differentiated into immature neurons, and finally they migrate into the DG where they mature and integrate in pre-existent circuits [95]. The pattern of protein expression varies depending on the developmental neural stage. NSCs express markers such as SOX2 and GFAP, whereas neuroblasts or immature neurons express DCX [96–98]. The results revealed that colistin does not affect NSCs as no changes in SOX2 or GFAP protein levels were observed. However, there was a reduction in the number of immature neurons [99], likely indicating a dysfunction in the short cell cycle division rate. Supporting these findings, other authors have suggested that antibiotic treatments, including polymyxins, could affect adult neurogenesis and reduce the number of immature neurons [100,101], leading to cognitive alteration. Indeed, various neuropsychiatric and neurodegenerative diseases, such as depression and Alzheimer's disease, have been associated with dysfunction of neurogenesis [102,103].

5. Conclusion

In summary, the findings of this study indicates that prolonged colistin treatment cause long-term effects related to cognitive impairment through oxidative stress accumulation, cell death, glial activation, dendritic spine loss, and neurogenesis impairment. These findings have significant implications for clinical practice as they highlight the need for caution when prescribing colistin, particularly in patients with conditions that might disrupt the BBB. This study suggests that alternative therapies should be considered to minimize the risk of neurotoxicity. Additionally, monitoring cognitive function in patients undergoing colistin treatment could help in the early detection and management of neurotoxicity.

Ethics statement

All procedures involving mice were done in accordance with European legislation and were approved by the Ethics Committee for Animal Experimentation of the University of Barcelona (CEEA) and accepted by the Department of Environment and Housing of the Generalitat de Catalunya with the license number 259/22.

Funding

This research was funded by the AEI of the Ministry of Science, Innovation and Universities [MICIU PCI2023–143362 and PID2021–124342OB-I00 to FR] [PID2021–123462OB-I00 to AC and CA]; Fundació Marató TV3 [ref 201829–10 to FR]; Grup de Recerca de la Generalitat de Catalunya [2021 SGR 00288 to CA]; CIBERNED [Grant CB06/05/2004 to AC]; the Institute of Neurosciences UB [CEX2021–001159-M to CA, AC and ME] and Spanish Ministry of Science and Innovation, Proyectos de Generación de Conocimiento grant [PID2021–122473OA-I00 to ACano and ME]. L. Guzman is supported by a Predocs-UB grant from the University of Barcelona. ACano acknowledges the support of the Instituto de Salud Carlos III (ISCIII) under Sara Borrell grant [CD22/00125[. M. Ettcheto is supported by a Serra Hunter contract [UB-LE-9115].

CRediT authorship contribution statement

Yolanda Cajal: Writing – review & editing, Conceptualization. **Marta Barenys:** Writing – review & editing, Validation, Investigation. **Antoni Camins:** Writing – review & editing, Resources, Project administration, Funding acquisition, Conceptualization. **Francesc Rabanal:** Writing – review & editing, Project administration, Investigation, Funding acquisition, Conceptualization. **Amanda Cano:** Writing – review & editing, Validation, Investigation, Funding acquisition. **Elena Sánchez-López:** Writing – review & editing, Validation, Investigation. **Ester Verdaguer:** Writing – review & editing, Methodology. **Carme Auladell:** Writing – review & editing, Methodology, Funding acquisition. **Antoni Parcerisas:** Writing – review & editing, Methodology, Investigation, Data curation. **Miren Ettcheto:** Writing – review & editing, Writing – original draft, Supervision, Resources, Project administration, Methodology, Investigation, Funding acquisition, Data curation, Conceptualization. **Laura Guzman:** Writing – review & editing, Writing – original draft, Project administration, Methodology, Investigation, Data curation.

Declaration of Competing Interest

The authors declare that they have no known competing financial interests or personal relationships that could have appeared to influence the work reported in this paper.

Acknowledgments

The authors acknowledge the team of the CCiTUB for their excellent technical support, and Leila Driouech from the Neurohistology and Advanced Microscopy Platform (UBNeuro) for her methodological assistance. The support of María de Maeztu (MDM): "Ayuda María de Maeztu Unit of Excellence CEX2021–001159-M / funded by MICIU/AEI / 10.13039/501100011033". Graphical abstract was created in BioRender. Guzman, L. (2025) https://BioRender.com/v72y884

Appendix A. Supporting information

Supplementary data associated with this article can be found in the online version at doi:10.1016/j.biopha.2025.117839.

References

[1] A. Miani, P. Piscitelli, R. Hodgton, M. Barchitta, A. Agodi, How antimicrobial resistance is linked to climate change: an overview of two intertwined global challenges, Int J. Environ. Res Public Health 20 (3) (2023) 1681, https://doi.org/10.3390/ijerph20031681.

[2] H. Kaba, E. Kuhlmann, S. Scheithauer, Thinking outside the box: Association of antimicrobial resistance with climate warming in Europe - A 30 country observational study, J. Hyg. Environ. 223 (1) (2019) 151–158, https://doi.org/10.1016/j.ijheh.2019.09.008.

[3] C.J. Murray, K.S. Ikuta, F. Sharara, L. Swetschinski, G. Aguilar, A. Gray, et al., Global burden of bacterial antimicrobial resistance in 2019: A systematic analysis, Lancet 399 (10325) (2022) 629–655, https://doi.org/10.1016/S0140-6736(21)02724-0.

[4] World Health Organization, Antimicrobial resistance. ⟨https://www.who.int/news-room/fact-sheets/detail/antimicrobial-resistance/⟩, 2023 (accessed 25 Jul 2024).

[5] World Health Organization, WHO list of critically important antimicrobials for human medicine. ⟨https://www.who.int/publications/i/item/9789241515528⟩, 2024 (accessed 25 Jul 2024).

[6] A.J. Kunz Coyne, A. El Ghali, D. Holger, N. Rebold, M.J. Rybak, Therapeutic strategies for emerging multidrug-resistant Pseudomonas aeruginosa, Infect. Dis. Ther. 11 (2) (2022) 661–682, https://doi.org/10.1007/s40121-022-00591-2.

[7] F. Rabanal, Y. Cajal, Recent advances and perspectives in the design and development of polymyxins, Nat. Prod. Rep. 34 (7) (2017) 886–908, https://doi.org/10.1039/C7NP00023E.

[8] F. Rabanal, A. Grau-Campistany, X. Vila-Farrés, J. Gonzalez-Linares, M. Borràs, J. Vila, et al., A bioinspired peptide scaffold with high antibiotic activity and low in vivo toxicity, Sci. Rep. 29 (5) (2015) 10558, https://doi.org/10.1038/srep10558.

[9] X. Liu, Y. Chen, H. Yang, J. Li, J. Yu, Z. Yu, Acute toxicity is a dose-limiting factor for intravenous polymyxin B: A safety and pharmacokinetic study in healthy Chinese subjects, J. Infect. 82 (2) (2021) 207–215, https://doi.org/10.1016/j.jinf.2021.01.006.

[10] T. Barichello, J.S. Generoso, A. Collodel, F. Petronilho, F. Dal-Pizzol, The blood-brain barrier dysfunction in sepsis, Tissue Barriers 9 (1) (2021) 1840912, https://doi.org/10.1080/21688370.2020.1840912.

[11] C. Dai, X. Xiao, J. Li, G.D. Ciccotosto, R. Cappai, S. Tanget, et al., Molecular mechanisms of neurotoxicity induced by polymyxins and chemoprevention, ACS Chem. Neurosci. 10 (1) (2019) 120–131, https://doi.org/10.1021/acschemneuro.8b00300.

[12] C. Dai, S. Tang, T. Velkov, X. Xiao, Colistin-induced apoptosis of neuroblastoma-2a cells involves the generation of reactive oxygen species, mitochondrial dysfunction, and autophagy, Mol. Neurobiol. 53 (7) (2016) 4685–4700, https://doi.org/10.1007/s12035-015-9396-7.

[13] C. Dai, J. Li, S. Tang, J. Li, X. Xiao, Colistin-induced nephrotoxicity in mice involves the mitochondrial, death receptor, and endoplasmic reticulum pathways, Antimicrob. Agents Chemother. 58 (7) (2014) 4075–4085, https://doi.org/10.1128/aac.00070-14.

[14] A. Subramanian, Evaluation of invitro antioxidant activity of Oxalis latifolia Kunth and its role in the treatment of neurodegenerative diseases, Ejpmr 6 (2) (2019) 349–356. ISSN: 2394-3211.

[15] M.E. Falagas, S.K. Kasiakou, Toxicity of polymyxins: A systematic review of the evidence from old and recent studies, Crit. Care 10 (1) (2006) 1–13, https://doi.org/10.1186/cc3995.

[16] H.N. Allbutt, J.M. Henderson, Use of the narrow beam test in the rat, 6-hydroxydopamine model of Parkinson's disease, J. Neurosci. Methods 159 (2) (2007) 195–202, https://doi.org/10.1016/j.jneumeth.2006.07.006.

[17] A. Bonetto, D.C. Andersson, D.L. Waning, Assessment of muscle mass and strength in mice, Bone Rep. 4 (2015) 732, https://doi.org/10.1038/bonekey.2015.101.

[18] J.F.O. Da Cruz, M. Gomis-Gonzalez, R. Maldonado, G. Marsicano, A. Ozaita, A. Busquets-Garcia, An alternative maze to assess novel object recognition in mice, Bio Protoc. 10 (12) (2020) e3651, https://doi.org/10.21769/BioProtoc.3651.

[19] A. Can, D.T. Dao, M. Arad, C.E. Terrillion, S.C. Piantadosi, T.D. Gould, The mouse forced swim test, J. Vis. Exp. (59) (2012) 3638, https://doi.org/10.3791/3638.

[20] K.Y. Kim, B.H. Kim, W.G. Kwack, H.J. Kwon, S.H. Cho, C.W. Kim, Simple and robust LC–MS/MS method for quantification of colistin methanesulfonate and colistin in human plasma for therapeutic drug monitoring, J. Pharm. Biomed. Anal. 30 (236) (2023) 115734, https://doi.org/10.1016/j.jpba.2023.115734.

[21] M.P. de S. Goldim, A.D. Giustina, F. Petronilho, Using evans blue dye to determine blood-brain barrier integrity in rodents, Curr. Protoc. Immunol. 126 (1) (2019) e83, https://doi.org/10.1002/CPIM.83.

[22] A. Manaenko, H. Chen, J. Kammer, J.H. Zhang, J. Tang, Comparison Evans Blue injection routes: Intravenous versus intraperitoneal, for measurement of blood-brain barrier in a mice hemorrhage model, J. Neurosci. Methods 195 (2011) 206–210, https://doi.org/10.1016/j.jneumeth.2010.12.013.

[23] C.A. Schneider, W.S. Rasband, K.W. Eliceiri, NIH Image to ImageJ: 25 years of image analysis, Nat. Methods 9 (7) (2012) 671–675, https://doi.org/10.1038/nmeth.2089.

[24] A. Parcerisas, L. Pujadas, A. Ortega-Gascó, B. Perelló-Amorós, R. Viais, K. Hino, NCAM2 regulates dendritic and axonal differentiation through the cytoskeletal proteins MAP2 and 14-3-3, Cereb. Cortex 30 (6) (2020) 3781–3799, https://doi.org/10.1093/cercor/bhz342.

[25] Riss T.L., Moravec R.A., Niles A.L., Duellman S., Benink H.A., Worzella T.J., et al. Cell Viability Assays, in: Arkossian S, Grossman A, Arkin M, et al., (Eds.), Assay Guidance Manual, Eli Lilly & Company and the National Center for Advancing Translational Sciences (2016). Bookshelf ID: NBK144065.

[26] H. Kim, X. Xue, Detection of Total Reactive Oxygen Species in Adherent Cells by 2',7'-Dichlorodihydrofluorescein Diacetate Staining. J Vis Exp, 2020, https://doi.org/10.3791/60682.

[27] R.P. Murmu, W. Li, A. Holtmaat, J.Y. Li, Dendritic spine instability leads to progressive neocortical spine loss in a mouse model of Huntington's disease, J. Neurosci. 33 (32) (2013) 12997–13009, https://doi.org/10.1093/cercor/bhz342.

[28] N. Haddad, M. Carr, S. Balian, J. Lannin, Y. Kim, C. Tothet, et al., The blood–brain barrier and pharmacokinetic/pharmacodynamic optimization of antibiotics for the treatment of central nervous system infections in adults, J. Antibiot. 11 (12) (2022) 1843, https://doi.org/10.3390/antibiotics11121843.

[29] T. Toda, S.L. Parylak, S.B. Linker, F.H. Gage, The role of adult hippocampal neurogenesis in brain health and disease, Mol. Psychiatry 24 (1) (2018) 67–87, https://doi.org/10.1038/s41380-018-0036-2.

[30] W. Das Neves, C.R.R. Alves, A.P. De Souza Borges, G. de Castro, Serum creatinine as a potential biomarker of skeletal muscle atrophy in non-small cell lung cancer patients, Front Physiol. 12 (2021) 625417, https://doi.org/10.3389/fphys.2021.625417.

[31] A. Goyal, P. Daneshpajouhnejad, M.F. Hashmi, K. Bashir, Acute kidney injury. Treasure Island (FL), StatPearls Publishing, 2024. Bookshelf ID: NBK441896.

[32] D.A. Bonilla, R.B. Kreider, J.R. Stout, Metabolic basis of creatine in health and disease: A bioinformatics-assisted review, Nutrients 13 (4) (2021) 1238, https://doi.org/10.3390/nu13041238.

[33] I. Wu, C.R. Parikh, Screening for kidney diseases: older measures versus novel biomarkers, Clin. J. Am. Soc. Nephrol. 3 (6) (2008) 1895–1901, https://doi.org/3(6):1895-901.

[34] S.S. Patel, M.Z. Molnar, J.A. Tayek, J.H. Ix, N. Noori, B. Benner, et al., Serum creatinine as a marker of muscle mass in chronic kidney disease: results of a cross-sectional study and review of literature, J. Cachex-.-. Sarcopenia Muscle 4 (1) (2013) 19–29, https://doi.org/10.1007/s13539-012-0079-1.

[35] S. De Rosa, M. Greco, M. Rauseo, M.G. Annetta, The good, the bad, and the serum creatinine: Exploring the effect of muscle mass and nutrition, Blood Purif. 52 (9-10) (2023) 775–785, https://doi.org/10.1159/000533173.
[36] A. Nigam, A. Kumari, R. Jain, S. Batra, Case Report: Colistin neurotoxicity: revisited, bcr2015210787, BMJ Case Rep. 2015 (2015), https://doi.org/10.1136/BCR-2015-210787.
[37] S. Wadia, B. Tran, Case Report: Colistin-mediated neurotoxicity, bcr2015210787, BMJ Case Rep. 2014 (2014), https://doi.org/10.1136/BCR-2014-205332.
[38] International mouse phenotyping consortium. Grip Strength. ⟨https://www.mousephenotype.org/impress/ProcedureInfo?action=list&procID= 1130/⟩, 2024 (accessed 25 Jul 2024).
[39] Mouse metabolic phenotyping centers. Grip Strength Test. ⟨https://www.mmpc.org/shared/document.aspx?id= 350&docType=Protocol/⟩, 2023 (accessed 25 Jul 2024).
[40] G. Özkan, Ulusoy Ş, S. Gazioğlu, M. Cansiz, K. Kaynar, D. Ari, Rhabdomyolysis and severe muscle weakness secondary to colistin therapy, Ren. Fail 34 (7) (2012) 926–929, https://doi.org/10.3109/0886022X.2012.684513.
[41] R.C. Radhakrishnan, S. Jacob, H.R. Pathak, V. Tamilarasi, Colistin induced neurotoxicity in a patient with end stage kidney disease and recovery with conventional hemodialysis, Open Urol. Nephrol. J. 8 (2015) 53–55, https://doi.org/10.2174/1874303X01509010053.
[42] P.K. Linden, S. Kusne, K. Coley, P. Fontes, D.J. Kramer, D. Paterson, Use of parenteral colistin for the treatment of serious infection due to antimicrobial-resistant Pseudomonas aeruginosa, Clin. Infect. Dis. 37 (11) (2003) e154–e160, https://doi.org/10.1086/379611.
[43] R. Bidgood, M. Zubelzu, J.A. Ruiz-Ortega, T. Morera-Herreras, Automated procedure to detect subtle motor alterations in the balance beam test in a mouse model of early Parkinson's disease, Sci. Rep. 14 (1) (2024) 862, https://doi.org/10.1038/s41598-024-51225-1.
[44] M.C. Orenduff, E.T. Rezeli, S.D. Hursting, C.F. Pieper, Psychometrics of the balance beam functional test in C57BL/6 mice, Comp. Med 71 (4) (2021) 302–308, https://doi.org/10.30802/AALAS-CM-21-000033.
[45] S.J. Wallace, J. Li, R.L. Nation, C.R. Rayner, D. Taylor, D. Middleton, et al., Subacute toxicity of colistin methanesulfonate in rats: comparison of various intravenous dosage regimens, Antimicrob. Agents Chemother. 52 (3) (2008) 1159–1161, https://doi.org/10.1128/aac.01101-07.
[46] W.J.M. Landman, R.M. Dwars, H.J. Keukens, B.J.A. Berendsen, Polymyxin E-1 (colistin sulphate) (neuro-)intoxication in young ostriches (Struthio camelus spp, Avian Pathol. 29 (6) (2000) 593–601, https://doi.org/10.1080/03079450020016841.
[47] C. Dai, J. Li, W. Lin, M. Sun, F. Wang, J. Li, Electrophysiology and ultrastructural changes in mouse sciatic nerve associated with colistin sulfate exposure, Toxicol. Mech. Methods 22 (8) (2012) 592–596, https://doi.org/10.3109/15376516.2012.704956.
[48] B. Lin, C. Zhang, X. Xiao, Toxicity, bioavailability and pharmacokinetics of a newly formulated colistin sulfate solution, J. Vet. Pharm. Ther. 28 (4) (2005) 349–354, https://doi.org/10.1111/j.1365-2885.2005.00666.x.
[49] C. Dai, J. Li, J. Li, New insight in colistin induced neurotoxicity with the mitochondrial dysfunction in mice central nervous tissues, Exp. Toxicol. Pathol. 65 (6) (2013) 941–948, https://doi.org/10.1016/j.etp.2013.01.008.
[50] B. Anroop, S.J. Nair, A simple practice guide for dose conversion between animals and human, J. Basic Clin. Pharm. 7 (2) (2016) 27–31, https://doi.org/10.4103/0976-0105.177703.
[51] S.L. Markantonis, N. Markou, M. Fousteri, N. Sakellaridis, S. Karatzas, I. Alamanos, et al., Penetration of colistin into cerebrospinal fluid, Antimicrob. Agents Chemother. 53 (11) (2009) 4907–4910, https://doi.org/10.1128/aac.00345-09.
[52] L. Jin, J. Li, R.L. Nation, J.A. Nicolazzo, Brain penetration of colistin in mice assessed by a novel high-performance liquid chromatographic technique, Antimicrob. Agents Chemother. 53 (10) (2009) 4247–4251, https://doi.org/10.1128/aac.00485-09.
[53] J. Wang, M. Yi, X. Chen, I. Muhammad, F. Liu, R. Li, Effects of colistin on amino acid neurotransmitters and blood-brain barrier in the mouse brain, Neurotoxicol Teratol. 55 (2016) 32–37, https://doi.org/10.1016/j.ntt.2016.03.004.
[54] T. Velkov, C. Dai, G.D. Ciccotosto, R. Cappai, D. Hoyer, J. Li, Polymyxins for CNS infections: Pharmacology and neurotoxicity, Pharm. Ther. 181 (2018) 85–90, https://doi.org/10.1016/j.pharmthera.2017.07.012.
[55] N. Zhang, L. Zhu, Q. Ouyang, S. Yue, Y. Huang, S. Qu, et al., Visualizing the potential impairment of polymyxin B to central nervous system through MR susceptibility-weighted imaging, Front Pharm. 12 (2021) 784864, https://doi.org/10.3389/fphar.2021.784864.
[56] S.W. Ryter, P.K. Hong, A. Hoetzel, J.W. Park, K. Nakahira, X. Wang, et al., Mechanisms of cell death in oxidative stress, Antioxid. Redox Signal 9 (1) (2007) 49–89, https://doi.org/10.1089/ars.2007.9.49.
[57] J.A. Klein, S.L. Ackerman, Oxidative stress, cell cycle, and neurodegeneration, J. Clin. Invest 111 (6) (2003) 785–793, https://doi.org/10.1172/JCI18182.
[58] T. Hussain, B. Tan, Y. Yin, F. Blachier, M.C.B. Tossou, N. Rahu, Oxidative stress and inflammation: What polyphenols can do for us? Oxid. Med Cell Longev. 2016 (2016) 7432797 https://doi.org/10.1155/2016/7432797.
[59] N. Khansari, Y. Shakiba, M. Mahmoudi, Chronic inflammation and oxidative stress as a major cause of age-related diseases and cancer, Recent Pat. Inflamm. Allergy Drug Discov. 3 (1) (2009) 73–80, https://doi.org/10.2174/187221309787158371.
[60] X.Z. Wang, H.H. Yang, W. Li, B.J. Han, Y.J. Liu, Studies on apoptosis in HeLa cells via the ROS-mediated mitochondrial pathway induced by new dibenzoxanthenes, N. J. Chem. 40 (6) (2016) 5255–5267, https://doi.org/10.1039/C6NJ00250A.
[61] J.E. Ricci, R.A. Gottlieb, D.R. Green, Caspase-mediated loss of mitochondrial function and generation of reactive oxygen species during apoptosis, J. Cell Biol. 160 (1) (2003) 65–75, https://doi.org/10.1083/jcb.200208089.
[62] C. Dai, C. Giuseppe, R. Cappai, Y. Wang, S. Tang, X. Xiao, et al., Minocycline attenuates colistin-induced neurotoxicity via suppression of apoptosis, mitochondrial dysfunction and oxidative stress, J. Antimicrob. Chemother. 72 (6) (2017) 1635–1645, https://doi.org/10.1093/jac/dkx037.
[63] S. Yılmaz, S. Küçükler, H. Şimşek, S. Aygörmez, F.M. Kandemir, Naringin protects against colistin-induced sciatic nerve damage by reducing oxidative stress, apoptosis and inflammation damage, J. Exp. Clin. Med 41 (1) (2023) 53–59, https://doi.org/10.52142/omujecm.41.1.9.
[64] Gergin, Ö. Gergin, İŞ, S.S. Pehlivan, O.C. Mat, I.T. Turan, A. Bayram, et al., The neuroprotective effect of mesenchymal stem cells in colistin-induced neurotoxicity, Toxicol. Mech. Methods 33 (2) (2023) 95–103, https://doi.org/10.1080/15376516.2022.2090303.
[65] G. Schiera, C.M. Di Liegro, G. Schirò, G. Sorbello, I. Di Liegro, Involvement of astrocytes in the formation, maintenance, and function of the blood–brain barrier, Cells 13 (2) (2024) 150, https://doi.org/10.3390/cells13020150.
[66] E.E. Benarroch, Astrocyte signaling and synaptic homeostasis, Neurology 87 (3) (2016) 324–330, https://doi.org/10.1212/WNL.0000000000003019.
[67] J. Wang, M. Yi, X. Chen, I. Muhammad, F. Liu, R. Li, et al., Effects of colistin on amino acid neurotransmitters and blood-brain barrier in the mouse brain, Neurotoxicol Teratol. 55 (2016) 32–37, https://doi.org/10.1016/j.ntt.2016.03.004.
[68] S. Salim, Oxidative stress and the central nervous system, J. Pharm. Exp. Ther. 360 (1) (2017) 201–205, https://doi.org/10.1124/jpet.116.237503.
[69] C.A. Massaad, E. Klann, Reactive oxygen species in the regulation of synaptic plasticity and memory, Antioxid. Redox Signal 14 (10) (2011) 2013–2054, https://doi.org/10.1089/ars.2010.3208.
[70] L.T. Knapp, E. Klann, Role of reactive oxygen species in hippocampal long-term potentiation: Contributory or inhibitory? J. Neurosci. Res 70 (1) (2002) 1–7, https://doi.org/10.1002/jnr.10371.
[71] A.C. Sartori, D.E. Vance, L.Z. Slater, M. Crowe, The impact of inflammation on cognitive function in older adults: Implications for health care practice and research, J. Neurosci. Nurs. 44 (4) (2012) 206–217, https://doi.org/10.1097/JNN.0b013e3182527690.
[72] M.A. Ahmad, O. Kareem, M. Khushtar, M.D. Akbar, R. Haque, A. Iqubal, et al., Neuroinflammation: A potential risk for dementia, Int J. Mol. Sci. 23 (2) (2022) 616, https://doi.org/10.3390/IJMS23020616.
[73] M. Karvanen, C. Malmberg, P. Lagerbäck, L.E. Friberg, O. Cars, Colistin is extensively lost during standard in vitro experimental conditions, Antimicrob. Agents Chemother. 61 (11) (2017) e00857-17, https://doi.org/10.1128/AAC.00857-17.
[74] L. Jiang, X.Y. Sun, S.Q. Wang, Y. Liu, L. Lu, W. Wu, et al., Indoxyl sulphate-TNFα axis mediates uremic encephalopathy in rodent acute kidney injury, Acta Pharm. Sin. 45 (2024) 1406–1424, https://doi.org/10.1038/s41401-024-01251-6.
[75] C.Y. Sun, J.R. Li, Y.Y. Wang, S.Y. Lin, Y.C. Ou, C.J. Lin, et al., Indoxyl sulfate caused behavioral abnormality and neurodegeneration in mice with unilateral nephrectomy, Aging (Albany NY) 13 (5) (2021) 6681–6701, https://doi.org/10.18632/aging.202523.
[76] M. Bobot, L. Thomas, A. Moyon, S. Fernandez, N. McKay, L. Balasse, et al., Uremic toxic blood-brain barrier disruption mediated by AhR activation leads to cognitive impairment during experimental renal dysfunction, J. Am. Soc. Nephrol. 31 (7) (2020) 1509–1521, https://doi.org/10.1681/ASN.2019070728.
[77] M. Karbowska, J.M. Hermanowicz, A. Tankiewicz-Kwedlo, B. Kalaska, T. W. Kaminski, K. Nosek, et al., Neurobehavioral effects of uremic toxin–indoxyl sulfate in the rat model, Sci. Rep. 10 (1) (2020) 9483, https://doi.org/10.1038/S41598-020-66421-y.
[78] S. Adesso, T. Magnus, S. Cuzzocrea, Indoxyl sulfate affects glial function increasing oxidative stress and neuroinflammation in chronic kidney disease: interaction between astrocytes and microglia, Front Pharm. 8 (2017) 370, https://doi.org/10.3389/fphar.2017.00370.
[79] S. Liabeuf, M. Pepin, C.F.M. Franssen, D. Viggiano, S. Carriazo, R.T. Gansevoort, et al., Chronic kidney disease and neurological disorders: are uraemic toxins the missing piece of the puzzle? Nephrol. Dial. Transpl. 37 (2) (2022) ii33–ii44, https://doi.org/10.1093/ndt/gfab223.
[80] M.F. Grill, R.K. Maganti, Neurotoxic effects associated with antibiotic use: management considerations, Br. J. Clin. Pharm. 72 (3) (2011) 381–393, https://doi.org/10.1111/j.1365-2125.2011.03991.x.
[81] K. Runge, C. Cardoso, A. de Chevigny, Dendritic spine plasticity: Function and mechanisms, Front Synaptic Neurosci. 28 (12) (2020) 36, https://doi.org/10.3389/fnsyn.2020.00036.
[82] M.M. Dorostkar, C. Zou, L. Blazquez-Llorca, J. Herms, Analyzing dendritic spine pathology in Alzheimer's disease: problems and opportunities, Acta Neuropathol. 130 (1) (2015) 1–19, https://doi.org/10.1007/s00401-015-1449-5.
[83] J.W. Swann, The spine loss paradox: Clues to mechanisms and meaning, Epilepsy Curr. 8 (6) (2008) 168–169, https://doi.org/10.1111/j.1535-7511.2008.00282.x.
[84] A. Kemp, D. Manahan-Vaughan, The Hippocampal CA1 region and dentate gyrus differentiate between environmental and spatial feature encoding through long-term depression, Cereb. Cortex 18 (4) (2008) 968–977, https://doi.org/10.1093/cercor/bhm136.
[85] K.A. Alkadhi, Cellular and molecular differences between area CA1 and the Dentate Gyrus of the hippocampus, Mol. Neurobiol. 56 (9) (2019) 6566–6580, https://doi.org/10.1007/s12035-019-1541-2.
[86] H. Hering, M. Sheng, Dendritic spines: structure, dynamics and regulation, Nat. Rev. Neurosci. 2 (12) (2001) 880–888, https://doi.org/10.1038/35104061.

[87] F. Engert, T. Bonhoeffer, Dendritic spine changes associated with hippocampal long-term synaptic plasticity, Nature 399 (6731) (1999) 66–70, https://doi.org/10.1038/19978.
[88] R. Kanjhan, P.G. Noakes, M.C. Bellingham, Emerging roles of filopodia and dendritic spines in motoneuron plasticity during development and disease, Neural Plast. 2016 (2016) 3423267, https://doi.org/10.1155/2016/3423267.
[89] M.E. Calhoun, M. Jucker, L.J. Martin, G. Thinakaran, D.L. Price, P.R. Mouton, Comparative evaluation of synaptophysin-based methods for quantification of synapses, J. Neurocytol. 25 (12) (1996) 821–828, https://doi.org/10.1007/BF02284844.
[90] E.F. Osimo, K. Beck, T. Reis Marques, O.D. Howes, Synaptic loss in schizophrenia: a meta-analysis and systematic review of synaptic protein and mRNA measures, Mol. Psychiatry 24 (2018) 549–561, https://doi.org/10.1038/s41380-018-0041-5.
[91] A.E.-D. El-Husseini, E. Schnell, D.M. Chetkovich, R.A. Nicoll, D.S. Bredt, PSD-95 involvement in maturation of excitatory synapses, Science 290 (5495) (2000) 1364–1368, https://doi.org/10.1126/science.290.5495.1364.
[92] W.C. Abraham, O.D. Jones, D.L. Glanzman, Is plasticity of synapses the mechanism of long-term memory storage? NPJ Sci. Learn 2 (4) (2019) 9, https://doi.org/10.1038/s41539-019-0048-y.
[93] Y. Ge, Z. Dong, R.C. Bagot, J.G. Howland, A.G. Phillips, T.P. Wong, et al., Hippocampal long-term depression is required for the consolidation of spatial memory, Proc. Natl. Acad. Sci. U. S. A. 107 (38) (2010) 16697–16702, https://doi.org/10.1073/pnas.1008200107.
[94] A.A. Coley, W.J. Gao, PSD-95 deficiency disrupts PFC-associated function and behavior during neurodevelopment, Sci. Rep. 9 (2019) 9486, https://doi.org/10.1038/s41598-019-45971-w.
[95] I. Sánchez-Gomar, N. Geribaldi-Doldán, C. Santos-Rosendo, C. Sanguino-Caneva, C. Carrillo-Chapman, O. Fiorillo-Moreno, et al., Exploring the intricacies of neurogenic niches: Unraveling the anatomy and neural microenvironments, Biomolecules 4 (3) (2014) 335, https://doi.org/10.3390/BIOM14030335.
[96] H. Hagihara, T. Murano, K. Ohira, M. Miwa, K. Nakamura, T. Miyakawa, Expression of progenitor cell/immature neuron markers does not present definitive evidence for adult neurogenesis, Mol. Brain 12 (2019) 1–6, https://doi.org/10.1186/s13041-019-0522-8.
[97] M.S. Vieira, A.K. Santos, R. Vasconcellos, V. Goulart, R.C. Parreira, A.H. Kihara, et al., Neural stem cell differentiation into mature neurons: Mechanisms of regulation and biotechnological applications, Biotechnol. Adv. 36 (7) (2018) 1946–1970, https://doi.org/10.1016/j.biotechadv.2018.08.002.
[98] L. Mu, L. Berti, G. Masserdotti, M. Covic, T.M. Michaelidis, K. Doberauer, et al., SoxC transcription factors are required for neuronal differentiation in adult hippocampal neurogenesis, J. Neurosci. 32 (9) (2012) 3067–3080, https://doi.org/10.1523/JNEUROSCI.4679-11.2012.
[99] A. Duque, J.I. Arellano, P. Rakic, An assessment of the existence of adult neurogenesis in humans and value of its rodent models for neuropsychiatric diseases, MolPsychiatry 27 (1) (2022) 377–382, https://doi.org/10.1038/s41380-021-01314-8.
[100] Y. Ye, H.Y.K. Tong, W.H. Chong, Z. Li, P.K.H. Tam, D.T. Baptista-Hon, et al., A systematic review and meta-analysis of the effects of long-term antibiotic use on cognitive outcomes, Sci. Rep. 14 (1) (2024) 4026, https://doi.org/10.1038/s41598-024-54553-4.
[101] F. Cordella, C. Sanchini, M. Rosito, L. Ferrucci, N. Pediconi, B. Cortese, et al., Antibiotics treatment modulates microglia–synapses interaction, Cells 10 (10) (2021) 2648, https://doi.org/10.3390/cells10102648.
[102] E.P. Moreno-Jiménez, M. Flor-García, J. Terreros-Roncal, J. Terreros-Roncal, A. Rábano, F. Cafini, et al., Adult hippocampal neurogenesis is abundant in neurologically healthy subjects and drops sharply in patients with Alzheimer's disease, Nat. Med 25 (4) (2019) 554–556, https://doi.org/10.1038/s41591-019-0375-9.
[103] P.S. Sung, P.Y. Lin, C.H. Liu, H.C. Su, K.J. Tsai, Neuroinflammation and neurogenesis in Alzheimer's disease and potential therapeutic approaches, Int J. Mol. Sci. 21 (3) (2020) 701, https://doi.org/10.3390/IJMS21030701.